Published in final edited form as:
Prog Energy Combust Sci. 2020 ; 76: . doi:10.1016/j.pecs.2019.100801.

Role of Firebrand Combustion in Large Outdoor Fire Spread

Samuel L. Manzello[1], **Sayaka Suzuki**[2], **Michael J. Gollner**[3], **A. Carlos Fernandez-Pello**[4]

[1]National Institute of Standards and Technology (NIST, USA, Japan)

[2]National Research Institute of Fire and Disaster (NRIFD, Japan)

[3]University of Maryland, College Park (USA)

[4]University of California, Berkeley (USA)

Abstract

Large outdoor fires are an increasing danger to the built environment. Wildfires that spread into communities, labeled as Wildland-Urban Interface (WUI) fires, are an example of large outdoor fires. Other examples of large outdoor fires are urban fires including those that may occur after earthquakes as well as in informal settlements. When vegetation and structures burn in large outdoor fires, pieces of burning material, known as firebrands, are generated, become lofted, and may be carried by the wind. This results in showers of wind-driven firebrands that may land ahead of the fire front, igniting vegetation and structures, and spreading the fire very fast. Post-fire disaster studies indicate that firebrand showers are a significant factor in the fire spread of multiple large outdoor fires. The present paper provides a comprehensive literature summary on the role of firebrand mechanisms on large outdoor fire spread. Experiments, models, and simulations related to firebrand generation, lofting, burning, transport, deposition, and ignition of materials are reviewed. Japan, a country that has been greatly influenced by ignition induced by firebrands that have resulted in severe large outdoor fires, is also highlighted here as most of this knowledge remains not available in the English language literature. The paper closes with a summary of the key research needs on this globally important problem.

1.0 Introduction

Large outdoor fires represent an increasing problem of global importance. Wildland fires that spread into urban areas, termed Wildland-Urban Interface (WUI) fires, are becoming more and more prevalent across multiple continents [1]. In many regions throughout the world, population centers are densely populated. In such areas, the risk exists for large urban fires. The USA has a long history of large urban fires such as the Great Chicago Fire in 1872, the Baltimore Fire in 1904, and fires following the San Francisco Earthquakes in 1906. In Japan, in particular, there is also a long history of such urban fires, such as the Meireki Fire in 1657, the fires following the 1923 Great Kanto Earthquake, the 1934 Hakodate Fire, and the 1976 Sakata Fire [2–3].

Corresponding author: samuelm@nist.gov.

In the developing world, there are many informal settlements. In both South Africa and the Philippines, these informal settlement fires have resulted in vast destruction and left many homeless. As an example, on March 2017, more than 2900 dwellings were destroyed that resulted in more than 9500 people homeless at the Imizamo Yethu informal settlement in South Africa.

A commonality in the rapid spread of large outdoor fires, such as WUI fires, urban fires, and informal settlement fires, are the production or generation of new, far smaller combustible fragments from the original fire source referred to as firebrands. In the case of WUI fires, the production of firebrands occurs from the combustion dynamics of vegetative and man-made fuel elements, such as homes and other structures. For urban fires and informal settlement fires, firebrands are produced primarily from man-made fuel elements.

An example of the importance of firebrand processes in WUI fires are collectively named the October Fire Siege of 2017, that burnt large portions of Napa and Sonoma counties in Northern California wine country. Videos show firebrand showers igniting vegetation and structures [4]. The largest of the fires in the siege, the Tubbs Fire, set the record at the time as the most destructive WUI fire in California history and ranked 3rd for the most-deadly WUI fire in California History [5]. Three other fires in the siege are also on the CALFIRE list of the Top 20 Most Destructive California WUI fires [6]. Altogether the fire siege consisted of a peak number of 21 major fires, killed a total of 43 people, burned over 100,000 hectares, forced the evacuation of 100,000 people, and destroyed an estimated 8,900 structures [5].

Later in December 2017 WUI fires also raged in Southern California. The largest one, the Thomas Fire (Ventura County) became at the time the largest WUI in California history, burning 114,000 hectares - more than the total area burned by all the fires in the October Fire Siege of 2017 [7]. If this was not enough, in November 2018, again in Northern California, the Camp Fire broke all the records becoming the most destructive fire to date [8] with a total of at least 86 people dead, an estimated 18,800 structures destroyed and over 153,000 hectares burnt [8], with most of the damage taking place within the first few hours. In all these fires there are many reports of firebrand showers igniting structures and vegetation. While two detailed examples of WUI fire destruction are provided for the USA, the interested reader is referred to a detailed report as part of an ISO TC92 Task Group that provides a global overview [2].

The 1934 Hakodate Fire in Japan produced more than 20 spot fires, with wind speeds of 20 m/s (72 km/hr) reported, resulting in more than 11,000 structures lost and 2,000 fatalities [9]. A more recent example of the importance of firebrand processes in urban fires occurred in the City of Itoigawa Niigata Prefecture, Japan on December 2016. Specifically, this fire broke out from a Chinese restaurant, and on the day of the fire, strong winds resulted in rapid fire spread. With the presence of an average wind speed of 9 m/s (32 km/hr), the fire quickly spread, resulting in the damage of 147 structures, with 120 destroyed [10]. After the March 2011 Great East Japan Earthquake, there were many urban fires as a result of the tsunami although these fires were not linked to firebrand processes [2].

The present paper provides a comprehensive literature summary on the role of firebrands on large outdoor fire spread. While previous reviews have explored aspects of the problem before [11–16], there has yet to be a focused review on the physical mechanisms governing firebrand propagation. Experiments, models, and simulations related to firebrand generation, lofting, burning, transport, deposition, and ignition of materials are presented. Previous work from Japan, a country that has been greatly influenced by ignition induced by firebrands that have resulted in severe large outdoor fires, is also highlighted here as most of this knowledge remains not available in the open, English language literature.

2.0 Overview of Physical Firebrand Mechanisms

In the most simplistic representation, fire development associated with firebrands may be divided into several sub-processes [12]: the generation of firebrands, their transport by plume lofting and drag forces with the wind, deposition onto and ignition of fuel beds by either flaming or smoldering, and the subsequent surface spread of the fire (these subsequent fire spread processes are not reviewed here). These sub-processes are illustrated in Figure 1 and described briefly below.

2.1 Firebrand Generation

Firebrands are primarily generated from burning wildland fuels (grasses, shrubs, trees) and wooden structures (structural members, shakes, shingles). They are produced when the burning fuels that carry the fire thermally decompose, lose structural integrity, and break into smaller burning pieces. These burning pieces may separate from the larger parent fuel due to the drag forces from the airflow surrounding the burning material and lofted by buoyant fire-induced plumes [17]. Although less common, firebrands can also be generated by power line interactions with trees or structures [18]. The characteristics of the firebrands depend on the type of the fuel (vegetation or structure), its morphology (geometry, size, porosity, density) and the intensity of the originating fire and buoyant plume characteristics. In addition to the physical characteristics of the fire the firebrands may be flaming or glowing (smoldering).

2.2 Firebrand Transport

The transport of the firebrands by the fire plume and ambient wind is the most studied aspect of the firebrand spotting process since the nature of the transport processes lends itself to simple calculation methodologies following Newton’s laws of motion (see Figure 2), although the combustion characteristics of the firebrand complicates these calculations. After the firebrands are generated, they are lofted by the fire plume and/or transported by ambient winds. An important but less studied aspect of the transport has been the accumulation of firebrands near obstacles, which has been only recently studied.

2.3 Ignition Induced by Firebrands

Perhaps the most important aspect of the firebrand problem is whether a firebrand or a shower of firebrands is capable of igniting a fuel bed after landing on it. Upon impingement on the fuel bed, firebrands may be in a flaming state, smoldering state, or they may be minimally reacting and just cooling. If enough energy is transferred from the firebrand to the adjacent fuel bed, the fuel will heat up and may start to pyrolyze while the firebrand loses

energy in the process. The heat released from the firebrand's reaction can also initiate self-sustained smoldering of the fuel bed that eventually may undergo transition into flaming. Alternatively, the pyrolyzate may quickly mix with ambient air, forming a flammable gaseous mixture near the firebrands which can directly ignite in the gas phase as a flame. This complex ignition process depends on several factors, including the characteristics of the firebrands upon landing (wood type, size, and state of combustion), the characteristics of the fuel bed on which the firebrand(s) lands (fuel type, temperature, density, porosity, void fraction, moisture content) and environmental conditions (wind speed, relative humidity, temperature). Naturally, a study of this complexity needs to be parameterized so that the effects of different parameters can be analyzed, and predictive models can be developed.

3. Detailed review on Current Knowledge for Firebrand Generation Processes

3.1 Firebrand Generation Studies

Firebrands are generated from structures such as houses and buildings as well as vegetation such as trees and shrubs. There is not yet a clear understanding of firebrand generation mechanisms from structures while a fundamental understanding of firebrand generation from vegetation has been obtained to some degree. Generation of firebrands is complex as many factors influence their generation, regardless of the source. Ambient wind speeds, fire-generated winds, and the geometry, distribution, and material composition of vegetation or structures all play a role. Without a comprehensive understanding of this process, it is not possible to fully parameterize the size, shape, mass, and energy characteristics of generated firebrands. Numerous experiments and several numerical studies have gathered data which will help to inform future predictive capabilities.

3.2 Firebrand Generation Knowledge Collected from Real Fires

As each real fire differs in its intensity and rate of growth, exposure conditions from the fire to elements that may generate firebrands are often difficult to determine. Parameters that may be of interest include the actual heat release rate (HRR) of the fire, the makeup of fuels involved, details of the suppression effort, if any, and ambient conditions such as the wind speed. During a real fire, it is difficult to know that information with the spatial and temporal resolution necessary to understand the generation of firebrands using current limited diagnostics. Most investigations are performed after the event has concluded. Controlled conditions in the laboratory, however, can offer limited ambient conditions that are easier to understand and draw trends from. Nonetheless, information obtained from actual fire events is invaluable to important validation and verification on all laboratory experiments.

Previous post-fire investigation reports mentioned firebrand generation from structures [19–21], with some recent reports including photos and videos of firebrands observed during these fires. While the majority of firebrands observed or reported during these investigations are relatively small in size, resembling a 'shower,' 'rain,' or 'blizzard,' of firebrands, some observations have noted lofted firebrands are large. Firebrands, however, may look larger or smaller than they actually are during observations taken in a critical incident, so care must be exercised with regard to interpretation of eyewitness accounts. The vast majority of small,

glowing firebrands are most likely hard to observe during daylight hours, and even during the night flaming firebrands will be easier to see.

Until recently, there has been very little effort to collect actual information on firebrands during post-fire investigations. After the Angora Fire in California, USA in 2007, a trampoline with holes burned by firebrands was observed. In this fire, the wildland fuels consisted of conifer forests of White Fire-Jeffery Pine. The opportunity was used to collect samples and the size of the holes was analyzed [22]. This was among the first information on firebrand size distributions produced in an actual WUI fire. More than 85 % of the holes had an area less than 0.5 cm^2, corroborating the assumption of the mostly small nature of firebrands. Another set of experiments were later conducted which confirmed that the sizes of holes melted through trampoline material indeed corresponded to the size of deposited glowing firebrands [22]. While it is difficult to say which holes were made from firebrands from structures or vegetation, the majority of firebrands were small. The same procedure was later used to investigate firebrand exposure in the Bastrop Complex Fire in Texas, USA in 2011 [23]. Seven trampolines were collected within the burned area, and holes in those trampolines were measured. The findings were similar - more than 90 % of ‘holes’ in 7 trampolines were less than 0.5 cm^2.

Firebrands have also been collected in several post urban fire investigations [10, 24–26]. In the Beppu-Fire in Japan on January 2010 (average wind speed of 10 m/s or 36 km/hr), firebrands were collected and compared with their travel distances [24]. The furthest travel distance was 1,160 m from the origin of the fire. Comparing this travel distance with the thickness, projected area, and mass of each firebrand, researchers reported a linear relationship between the projected area and mass of a firebrand, and a qualitative relationship between the maximum length transported and the projected area. They did not find any particular correlations between the travel distance and characteristics of firebrands. Another post-fire investigation reported that the size and mass of firebrands collected from the fires under low wind speeds were also linearly correlated [25].

In a post-fire investigation of the Itoigawa-City Fire in Japan on December 2016, firebrands were collected after the fire and the size and the mass of each firebrand were measured [10, 26]. At least 10 spot fires were reported. While the largest firebrands found in the fire had a mass of 114 g, the majority of collected firebrands had a projected area less than 10 cm^2, similar to data from the Beppu-City Fire (shown in Figure 3) and structure combustion experiments described later. If the origin of the firebrands was assumed or known, the distance from the origin of the fire could be compared with the characteristics of collected firebrands. The Tachikawa number (Ta), representing the ratio of aerodynamic forces to gravitational forces, was used to correlate these findings by treating firebrands as windborne debris, assuming size and density remain constant [27]:

$$\mathrm{Ta} = \frac{\rho_\infty U^2 A_{proj}}{2 m_F g} \tag{1}$$

where ρ_{air} is the density of ambient air, U is an average wind speed experienced by the particle, m_F is the mass of a firebrand, A_{proj} is the projected area of a firebrand, and g is the

gravitational acceleration. The larger the Tachikawa number, the further a windborne debris, or firebrand, can travel. While the approach is promising, the results were not conclusive as it was difficult to determine the precise origin of individual firebrands. The same issue arose in post-fire investigations of the Beppu-City fire [24]; however, an experiment burning a three-story school [28] had more success owing to its clear, single fire origin (the school building). This shows the difficulty in finding the exact travel distance and firebrand source location in real fires.

It must be emphasized that it is important to gather firebrand information from real fires. While obtaining firebrand data from real fires always comes with unknown parameters, such as building materials, the precise fire origin, and the exact fire size, this information is still critical to be able to yield insights into the overall physics and provide validation data only actual fire events may provide.

3.3 Understanding Firebrand Generation from Vegetation – Laboratory Studies

Firebrand production from vegetation has been studied, both theoretically and experimentally in the laboratory and in the field. Early laboratory experiments to investigate firebrands from full-scale tree combustion were performed by using Douglas-fir trees (*Pseudotsuga menziesii)* 5.2 m in height with a 3 m wide maximum girth at the National Institute of Standards and Technology (NIST) [17]. No wind was applied, and firebrands were collected by pans filled with water. Prior experiments of Douglas-fir tree combustion, conducted not for the purposes of firebrand collection, but for heat-release rate measurements, suggested three regimes of combustion based on tree moisture content (MC): a regime which was not possible to sustain combustion, a transition regime where trees would partially combust, and a vigorous combustion regime [29]. These MC regimes were used as a basis for the firebrand tree combustion experiments. Trees with 50 % MC partially burned with no firebrands produced while the trees with 18 % MC were engulfed in flames after only 20 s after ignition, producing numerous firebrands. Firebrands collected from trees with 18 % MC had cylindrical shapes with an average size of 4 mm in diameter and a length of 53 mm. The surface area was calculated and plotted against mass, shown in Figure 4. This relationship is useful when comparing area-based measurements of firebrands to the mass, which is more closely related to energy content, and its influence on ignition. In addition, another experimental series was performed with Douglas-fir trees *(Pseudotsuga menziesii)* 2.4 m in height with a 1.5 m wide maximum girth [17]. The average size of firebrands was 3 mm in diameter and a length of 40 mm. This relationship was later studied using scaling analyses between firebrand mass and projected area for cylindrical firebrands, finding that the surface area should be related in power-law form to the mass to the 2/3 power [30]. While useful, this power law relationship should be evaluated for a more diverse set of fuel types.

Korean pine *(Pinus koaiensis)*, which is native to China, Japan, and Korea, was combusted at the Building Research Institute (BRI) Fire Research Wind Tunnel Facility (FRWTF) to investigate the difference in firebrand production from different tree species [31]; no wind was applied. The height was kept constant at 4.0 m, and pans with water were placed around the tree for the firebrand collection. With no data available for Korean pine combustion and

MC, experiments were performed with different MC. In order to have Korean pine combusted completely with a significant number of firebrands produced, it was found that MC had to be kept below 35 % without any wind applied. The burn progressed somewhat sporadically, taking more than 2 minutes to complete. This was almost double duration for Douglas-fir trees (50 s to 60 s). Firebrands were found to be cylindrical in shape with an average diameter of 5 mm and average length of 34 mm. The mass and size of firebrands is also shown in Figure 4.

The total mass of firebrands produced from each tree size was normalized with the mass lost from the tree during the burn as well as initial mass of the tree, shown in Figure 5. While Douglas-fir trees showed a decrease in firebrand production (almost half) with an increase in tree height (almost double), Korean pine trees produced a larger ratio of mass of firebrands compared with Douglas-fir trees. With the ratio of burnable parts (needles and twigs) of Douglas-fir and Korean pine being similar, this reflects the difference of burning behavior between the two species. As mentioned previously, it took more than 2 min for Korean pine to burn completely while Douglas-fir trees burned out completely in 50 s to 60 s for both heights tested. Douglas-fir trees also have a fuller, less open structure than Korean pine. The (HRR) estimated during the experiments in each case showed that, as for similar MC, Douglas-fir burns produced higher HRR than Korean pine [32–33]. The authors concluded that, as most of firebrands produced or collected in this series were relatively small, the more intense fire plume from higher HRR Douglas fir burns might have consumed smaller firebrands completely before collection [31].

While leaves from trees can often be considered to burn out before becoming firebrands, leaves on the ground may behave as (flaming) firebrands, especially under windy conditions. Firebrands from leaves have been observed during flame spread experiments with leaves under a 2 m/s wind and an 18-degree slope. When wind was higher than 4 m/s, spotting fires by flaming leaves was also observed [34].

3. 4 Understanding Firebrand Generation from Vegetation – Field Studies

A series of field experiments in the Pinelands National Reserve, New Jersey, in the USA has been performed as a part of prescribed burns over several years, from 2013 to 2016. Firebrands were collected during the prescribed burns, and efforts were made to link firebrand data with vegetation, velocity (wind and firebrands), combustion state (burning or non-burning), travel distance (distance from the fire front location) and fire intensity (fire size). Unfortunately, the collection method and the obtained characteristics of firebrands were changed over years, which made comparison of firebrands rather difficult. In 2013, firebrands were collected in three locations using pans filled with water and a thin plastic layer on top through which only reacting firebrands would be expected to penetrate [35]. They distinguished firebrands from bark and those from twigs. Most bark fragments had a 1 mm to 2 mm thickness, while 70 % of branch fragments collected had diameters between 2 mm to 4 mm. The thickness and the cross-sectional area of firebrands were compared with data from [17,31] in Figure 6, which shows the data from experiments in the laboratory matched well with those from the field. Prescribed burns were performed in the following

years, and firebrands were also collected [36]. This data also matches with firebrand data from the Angora Fire [22].

Another set of prescribed fires were performed in 2016 with some improved firebrand measurement technology [37]. Pans filled with water were still used to collect deposited firebrands, but without a plastic film. The average firebrand flux collected in the previously-described pans was correlated to the fire intensity which produced these firebrands, ranging between 7.35 MW ± 3.48 MW and 12.59 MW ± 5.87 MW. The average firebrand flux was determined based on the total number of firebrands collected divided by the time over which they were collected–starting with the time the first firebrand deposited in the containers to the last firebrand deposition in the containers. Video recording revealed that the peak firebrand flux lasted for only one or two minutes. As expected, higher fire intensities produced more firebrands, peaking at 0.82 m^{-2} s^{-1} to 1.36 m^{-2} s^{-1}. A summary of measured firebrand densities from these experiments is shown in Table 1.

3.5 Understanding Firebrand Generation from Vegetation – Modelling Studies

Modeling firebrand generation from vegetation, such as a tree, first requires a mathematical description of the shape of the tree, followed by a model for the mechanical strength of tree branches, and eventually, degradation of the mechanical strength over time. Description of the geometry of a tree was first introduced by Mandelbrot [38] as a fractal geometry, and Collin *et al.* [39] incorporated this concept into computational methods. They assumed a geometry with no leaves and where one branch splits only into two. The ratio of mass between two successive branches (m_{i+1} and m_i, respectively) was described by the fractal similarity:

$$\frac{m_{i+1}}{m_i} = \frac{\rho_s V_{i+1}}{\rho_s V_i} = \frac{\rho_s\left[n_{i+1}\left(\frac{\pi}{4}D_i^2+1\right)AD_{i+1}\right]}{\rho_s\left[n_i\left(\frac{\pi}{4}D_i^2\right)AD_i\right]} = \left(\frac{n_{i+1}}{n_i}\right)\left(\frac{D_{i+1}}{D_i}\right)^3 = 2\left(2^{-\frac{1}{2}}\right)^3 \approx 0.71 \quad (2)$$

This equation shows that the mass of the branch (m) decreases as the nominal diameter decreases (D), with ρ_s the solid density, V the branch volume, and A the aspect ratio. This equation may be different if the assumed tree has either leaves or one branch splitting into more than two.

In Barr and Ezekoye [40] the pyrolysis and oxidation degradation process for a woody element was assumed; as pyrolysis happens at lower temperature, pyrolysis was first considered, with a decrease in the density and strength of branches but no associated oxidation or regression of the element. In a second step, a constant density and strength were assumed and shape and size changes were considered [40]. Breakage was assumed to occur either when the branch becomes fragile due to the decrease of strength from pyrolysis or when the branch becomes fragile due to the diameter reduction from oxidation.

Assuming a cylindrical branch, the decrease of branch diameter (D) by oxidation can be described as a function of time:

$$\frac{dD}{dt} = -2\gamma\alpha_a\frac{\rho_\infty}{\rho_s}\ln(1+B)\left(\frac{U}{v_a}\right)^{\eta}Pr^{1/3}D^{\eta-1} \tag{3}$$

where B is the mass transfer number, Hilpret's correlation was assumed for the Nusselt number, and γ and η are constants from the Reynolds number included in that correlation. The thermal diffusivity, the density, and the kinematic viscosity of air are represented as α_a, ρ_a, and v_a. If the external flow U is constant, it is possible to integrate over the oxidation time t_{ox} from the initial diameter (D_o) to later diameter (D_{ox}):

$$\frac{D_{ox}}{D_o} = \left[1 - 2(2-\eta)\frac{\rho_a}{\rho_s}\ln(1+B)\overline{Nu_{D_o}}\left(\frac{t_{ox}}{\frac{D_o^2}{\alpha_a}}\right)\right]^{\frac{1}{2-\eta}} \tag{4}$$

A given branch i is subject to a different load, and the diameter reaches the critical diameter at which the branch fractures. Each branch is subjected to the force from its own weight and a drag force from a plume. It is assumed that the external flow velocity is in the opposite direction of the gravitational force. Therefore, the bending moment, M, at the base of branch i can be described as:

$$M_i = \frac{L_i}{2}\cos\theta_i\left[\frac{1}{2}\rho_a U^2 C_d D_i L_i - \rho_s\frac{\pi}{4}D_i^2 L_i g\right] \tag{5}$$

where C_d is the drag coefficient. The maximum flexural stress, σ, can be calculated as:

$$\sigma = \frac{32M}{\pi D^3} = \frac{8L^2\cos\theta}{\pi D^2}\left[\rho_a U^2 C_d - \rho_s\frac{\pi}{2}Dg\right] \tag{6}$$

The diameter of the branch should reach the critical diameter of branch D_{cr} upon reaching the critical flexural stress σ_{cr}. Inserting Eq. 6 into the polynomial for D/Do provides:

$$\left(\frac{D_{cr}}{D_o}\right)^2 + 2\left(\frac{2\rho_a g D_o A^2\cos\theta}{\sigma_{cr}}\right)\left(\frac{D_{cr}}{D_o}\right) - \left(\frac{\frac{8}{\pi}\rho_a U^2 C_d A^2\cos\theta}{\sigma_{cr}}\right) = 0 \tag{7}$$

where A is defined as the aspect ratio (L/D_o). The characteristic stress associated with the weight of the branch itself and the characteristic stress associated with drag on the branch are defined as $\sigma_w = 2\rho_a g D_o A^2\cos\theta$ and $\sigma_d = \frac{8}{\pi}\rho_a U^2 C_d A^2\cos\theta$ respectively, and the failure criteria can be described in a simple form:

$$\frac{D_{cr}}{D_o} = \left[\left(\frac{\sigma_w}{\sigma_{cr}}\right)^2 + \left(\frac{\sigma_d}{\sigma_{cr}}\right)\right]^{1/2} - \left(\frac{\sigma_w}{\sigma_{cr}}\right) \tag{8}$$

If $\sigma_w << \sigma_{cr}$ or $\sigma_d/\sigma_w >> \sigma_w/\sigma_{cr}$, the dependence on intimal diameter can be negligible. Therefore, the equation can be simplified as:

$$\frac{D_{cr}}{D_o} = \left(\frac{\sigma_d}{\sigma_{cr}}\right)^{1/2} \tag{9}$$

The time evolution of the oxidizing branch can be expressed in a non-dimensionalised form by using σ_w as a replacement for the initial diameter D_o. Hilpert's correlation for $\overline{Nu_{D_o}}$ can then be introduced alongside appropriate constants for $40 < \mathrm{Re}_D < 4000$ [40]:

$$\frac{D_{ox}}{D_o} = \left[1 - \frac{t_{ax}}{\tau}\left(\frac{\sigma_w}{\sigma_{cr}}\right)^{-3/2}\right]^{\frac{2}{3}}, D_{ox} > D_o \tag{10}$$

where the time constant τ was defined as:

$$\tau = \left[3\gamma\frac{\rho_a}{\rho_s}\ln(1+B)\left(\frac{U}{\upsilon}\right)^{1/2} Pr^{1/3}\left(\frac{2\rho_a g A^2 \cos\theta}{\sigma_{cr}}\right)^{3/2}\right]^{-1} \tag{11}$$

The branch is then assumed to break off when Eqs (8) and (10) intersect.

This data was then used as input for firebrand transport. Barr and Ezekoye [40] performed three-point bending experiments on thermally degraded yellow poplar (*Liriodendron tulipifera*) dowels using an oven for heating with different densities and found a linear relationship between flexural strength and density. This relationship is further confirmed with poplar, birch, and oak using heating provided by a diffusion flame by Caton [41]. They also provide a simplified nondimensional relationship between degradation of wooden dowels and the flexural strength required for fracture, $F_{\max:}$:

$$\frac{F_{\max:} L_0 \upsilon_{RT}}{E_L D_0^3}\left(\frac{\rho_0}{\rho_S}\right) \sim \frac{\alpha \dot{m} \rho_\infty}{P_\infty D_0^3 \rho_0} \tag{12}$$

where L_0 and D_0 are the initial length and diameter of the dowel, υ_{RT} is the Poisson's ratio in the radial plane R and in the transverse direction T in the RTL coordinate system, α is the species' thermal diffusivity, $\dot{m}$ is the mass loss rate, E_L is the modulus of elasticity in the longitudinal direction, ρ_s is the density of wood cell wall material, and P_∞ and ρ_∞ are the ambient pressure and density, respectively. The first parameter can be interpreted as the ratio of the average burning rate of the material to its scaled mechanical stiffness, and the second a non-dimensional representation of the recoverable plastic strain in the transverse direction of the dowels. Ultimately two failure modes are found, one dominated by the fracture strength of larger members and the other by the burning rate for smaller members. A fractal approach to modeling a tree has also been used in other work, such as estimating the radiant heat from a tree [32].

Tohidi *et al.* [30] modeled firebrands based on experimental observations by Manzello *et* al. [17,31], assuming a cylindrical shape. It was assumed that a branch or a twig is broken off from a larger branch by shear stresses related to bending due to weight or drag. This is also used as input data for transport studies.

The challenge for these modeling studies is simply a lack of experimental data to be able to validate these models over a broad parameter space. It cannot be overstated that more experimental data is required to guide future modeling efforts.

3.6 Understanding Firebrand Generation from Structures

3.6.1 Wood crib as a surrogate—As a part of attempts towards understanding firebrand production and providing validation data for future simulations, wood cribs have been used as surrogates for buildings [42]. Hayashi and Iwami investigated the effect of the size of wood cribs under different wind conditions and its effect on the mass of firebrands collected downstream. Wood cribs were all 450 mm in height with square widths and lengths of 1000 mm, 1500 mm, and 2000 mm (Table 2). The mass of the wooden cribs and number of firebrands produced were tracked as a function of time, with the later sampled every 30 s. Pans with water and an overhead CCD camera were placed at three downstream locations for each experiment. A total of 2095 firebrands were collected for all the experiments performed, with the majority of firebrands having a mass between 0.005 g to 0.01 g. As the wind speed increased, the average mass as well as the production rate of firebrands collected were also increased slowly at lower wind speeds then rapidly at higher wind speeds shown in Figure 7. The firebrand production rate also experienced a sudden increase near the end of experiments when the wood crib collapsed.

3.6.2 Structure Combustion Studies—Efforts to understand firebrand generation from building structures started with Vodvorka's residential house burn experiments [43–44]. Five residential houses were burned [43], and firebrands were collected using polyurethane sheets placed downwind from the houses, along with other data such as radiation, burning time, and fire spread rates. Five houses were tested in these experiments; three out of five were standard frame construction with wood sidings, one was asphalt siding applied over sheet rock, and the other was a brick veneer over a wood frame. Firebrands burned though the polyurethane sheets and left holes that were used for the measurements. The total number of firebrands collected from these structure fires was 4748. Eighty-nine percent of firebrands collected in these experiments were found to be smaller than 0.23 cm^2. The largest number of firebrands were observed to be produced upon the roof collapse. Vodvorka [43–44] also produced another study with eight structures, five of which were two-and-a-half-story wood houses with varying construction types. Information on the state of burning and firebrand production were collected in the same manner. In total, 2357 firebrands were collected. 85% of the firebrands were less than 0.23 cm^2 in projected area. Only 14 firebrands had projected areas larger than 14.44 cm^2 in three experiments. In both experimental series, ambient wind speeds were not provided. These experiments showed that firebrands with projected area of less than 0.23 cm^2 were significant.

Waterman [45] investigated firebrand generation from roof assemblies with three different sheathings (2 inch thick fir, 1 inch thick yellow pine and 5/16 inch thick plywood) and sidings (including no sidings applied, wood shingles, asphalt shingles, roll roofing and cement-asbestos shingles), and pitch (inclination) as well as inside pressure induced by applying wind from underneath. Firebrands were collected by meshes in water pools placed around the roof assemblies. Firebrands produced in this experimental series were in the

glowing state. It was found that wood shingles produced far more firebrands than any other material. It was also mentioned that wind induced pressure had the most effect on firebrand production; the higher the total pressure was, the larger number and larger mass of firebrands were produced.

Many researchers have used containers filled with water for firebrand collection. Without water, firebrands continue combustion to burn and it is possible for firebrands to become ash by the time of collection. Experiments in BRI's FRWTF confirmed some of these observations. Five experiments were performed under different conditions such as wind speeds or materials used for the mock-up structure built for the experiments [46]. Firebrands were collected in three out of five experiments. Two pans, one with water (wet pan) and the other without water (dry pan), were used to collect firebrands in two of those experiments. Pans were placed 1 m downstream from the house symmetry. All experimental conditions are shown in Table 3. The average mass of firebrands collected in wet pans was smaller than those collected in dry pans yet the total number of firebrands from wet pans was larger than those from dry pans. The higher wind speed produced the largest firebrands, along with a large number of small firebrands with a projected area up to 2 cm^2. The number of firebrands in the pans was counted every five minutes via video recording in one case. It was observed the largest number of firebrands was produced and deposited in both pans upon flashover in the structure. Increases in firebrand production were also noted upon wall or roof collapse and start of flame ejections out of the structure though the roof or wall.

A three-story wooden school burn with the dimension of 50 m (L) × 16 m (W) × 15 m (H) was conducted in Tsukuba, Japan to study fire safety of wooden school buildings [28,47]. Along with heat flux, temperature, and fire prevention strategies tested, firebrands were also collected after the experiment [28,47]. The distance from the origin of fire was measured along with the characteristics of firebrands. The size and the mass of firebrands for each size class and for each location showed linear relationships regardless of size class and location (namely, the mass of firebrands is proportional to the projected area of firebrand). They found the values of slope decreased as the travel distance increased and as the size of firebrands became smaller. More than 60 % of firebrands were between the size of 1 cm to 3 cm regardless of the location.

While it is interesting to burn an entire structure in order to obtain firebrands, it is hard to control all the parameters which may or may not affect the production. Hence, a systematic series of experiments were conducted with decreasing scale and complexity: a real-scale structure, a simple full-scale structure combustion experiment, full-scale building components combustion experiments, and bench-scale building components [48–53] combustion experiments. In all experiments, firebrands were collected in pans with water, and the projected area and the mass of each firebrand were measured in the same manner for all experiments in order to keep consistency to directly compare results.

First, a real-structure burn experiment was conducted in California, USA, as part of firefighter training [48]. Firebrands were collected in two locations, 4 m and 18 m from the structure. An average wind velocity of 6 m/s was measured during the burn. Firebrands were found to be made from wood and tar paper. All the firebrands collected in this burn had a

mass of less than 1 g and the projected area of most of firebrands were less than 10 cm^2. The effect of fire suppression, as water was applied by firefighters during the burn, was not known, but could have influenced results. As compared to the data of Vodvorka [43], firebrand projected areas were generally larger. This may be due to the difference of materials as well as the collection methods used (sheets versus water pans).

Subsequently, an experiment with a simpler full-scale structure was conducted in BRI's FRWTF [49]. This structure was made simply from OSB and wood studs with the dimensions of 3 m (W) × 4 m (L) × 4 m (H). Mass loss of the structure was also measured during the burn and the peak fire intensity was estimated to be 1.76 MW/m^2. The applied wind speed was 6 m/s, which was selected to be similar to the wind speed in the previous, more complex real-scale structure burn experiment [48]. More than 90 % of firebrands weighed less than 1 g and had less than 10 cm^2 projected area. Comparison with the firebrands from the real-scale structure in [48] showed that the firebrands from this study were slightly heavier in mass, at a given projected area. Materials used for the structure burned in this study were OSB/wood studs with no siding applied while the structure that was burned in Dixon, CA [48] was fitted with wood siding, tar paper, and plywood. It was suggested that this variety of materials in the structure might be responsible for lighter firebrands.

As a further simplification, full-scale building component combustion experiments were also performed with wall assemblies as well as roofing assemblies [50–52]. A repeatable ignition method was developed. After the assembly was placed, a flame was applied by using a 30 kW T-shaped burner for 10 min. The ignition source was applied without wind in order to ensure the same amount of heat for ignition. Once the assembly was ignited, the burner was tuned off, and then the wind at 6 m/s or 8 m/s was applied. This method produced a similar size and mass of firebrands in repeated experiments. First this method was used to the wall assemblies [50] and then roofing assemblies [51]. Firebrands from simple wall (re-entrant corner) assemblies, made from OSB and wooden studs, under different wind speeds were investigated and the firebrands under 8 m/s (higher wind speed used) had larger projected areas than under 6 m/s winds [50]. Nonetheless, most of the firebrands collected in this study also had less than 1 g in mass and 10 cm^2 projected area. For the roofing assemblies made from simple OSB and wooden studs, a similar experiment was performed using the same method [51]. A significant number of firebrands were found to be within the same range as those from the wall assemblies. Roofing assemblies produced the larger number of firebrands between 0 cm^2 to 0.9 cm^2 projected area. Compared with the wall assembly, where higher wind speeds produced larger firebrands, the roof assemblies produced larger firebrands at lower wind speeds. The peak of the projected areas for both assemblies was 0 cm^2 to 0.9 cm^2, yet a larger number of firebrands were obtained for 8 m/s rather than 6 m/s, reducing the ratio between mass and projected area more sharply than 6 m/s. Average projected area and mass were compared with roofing assembly the smallest, then Itoigawa-City Fire data [10], then wall assembly data. Despite a change in scale and configurations, the firebrand data in these experiments matched data from real events well. This same experimental method was applied to investigate firebrand production from cedar shingle sidings on wall assemblies [52]. These firebrands had a larger projected area than those from OSB. Firebrands made from tar paper, part of the assembly, were also collected and had a

lighter mass than other firebrands collected. The peaks of the size distributions of firebrands collected from the wall assemblies with cedar siding shifted to the smaller size compared with the ones with no siding.

Finally, the wind effect on firebrand generation from building components was investigated carefully at the bench-scale [53]. This bench-scale experimental method was newly developed with an aim to produce firebrands similar to those from full-scale building components. The comparison of firebrand data from a series of experiments under the same wind speed, 6 m/s, is shown in Fig. 8. The same ignition method as described earlier (a T-shaped burner) was applied, but for shorter ignition time (5 min compared with 10 min). The mock-up assemblies were half the length and half the width of the full-scale experiments. The small-scale study showed that the projected area of firebrands, A_{proj} has a linear relationship with their mass:

$$m_F = \rho_F d A_{proj} \tag{13}$$

where d is an approximate thickness of the firebrand and ρ_F their density. Assuming firebrands had the same density, they concluded that the thickness of firebrands was affected by the wind speed, as the higher wind speed meant a stronger wind force which would result in higher stresses capable of fracturing larger-thickness components. This relationship was compared with the literature [49–50], and the trend was similar.

Clearly, firebrands are produced when structures are combusting. Their nature is not yet fully known; however, it has been shown that these firebrands can be generated at multiple scales, even in the laboratory. While the fire plume and wind are believed to be major factors in firebrand production, observations of an increased rate of firebrand production during structural collapse and firefighting operations point to other effects that, as of yet, are not well documented. A key feature missing from nearly all the firebrand generation experimental studies is quantification of the heat release rate of the various building components and actual structures. While this is very difficult to obtain such information experimentally, more efforts are needed here.

4. Detailed review on Current Knowledge for Firebrand Transport Processes

After firebrands are generated, they are lofted by the fire plume and/or transported by ambient winds. Plume correlations or CFD simulations for axisymmetric and line fires [54–61] can be used in conjunction with drag coefficients to determine the lofting (vertical) force applied to a firebrand. The lateral (horizontal) force components are determined in a similar way based on the wind's velocity profile. These calculations, however, require information about the plume characteristics, wind profile, and firebrand thermo-chemical properties variations [15]. Pioneering work in this aspect of the problem was conducted by Tarifa *et al.* [54,62] that experimentally determined drag and burning rates of spheres, cylinders, and plates of various woods. A key conclusion of this work was that firebrands could be assumed to fall at their terminal velocity, as this was reached quickly in comparison to the particle's longer burning time. This work was later extended by Lee and Hellman [63], Muraszew *et*

al. [64], and Albini [65–67], who considered lofting of firebrands by line thermals and fire plumes and provided methods for simulating their transport and burning rate, ultimately resulting in practical models for the maximum distance a firebrand could spot. These early works have been followed by several theoretical and experimental studies of the transport of firebrands addressing different aspects of the problem [68–74]. These researchers applied different models of a buoyancy-dominated plume to calculate lofting and subsequent wind transport of firebrands of different shapes (spheres, cylinders, disks). Himoto and Tanaka [70], Koo *et al.* [71], Kortas *et al.* [75], and Sardoy *et al.* [73–74] studied the transport of firebrands using different CFD models to predict the plume characteristics and firebrand transport. A model for firebrand lofting and transport has been included in the CFD model FIRETEC [72] by Koo *et al.* [71]. FIRETEC is a physics-based wildand fire model [72]

Another far less cited and well-known approach involved calculating concentration distributions of aerosols (pollutants) under the assumption that firebrands are small enough to be considered such types of pollutants [76]. Kamei also investigated several fires and plotted the number of spot fires versus distance and wind speeds [77]. Yet another important but less studied aspect of the transport has been the accumulation of firebrands near obstacles, which has been only recently studied experimentally [78]. There have also been studies examining firebrands and measurements such as firebrand flux (firebrands per unit area time) from a controlled burn fire [37].

4.1 Firebrand Trajectories

Calculating the trajectories of the firebrands follows directly from application of Newton's laws of motion [15]. The formulation of the problem follows the well-established ballistic equations with the added complexity that the firebrands maybe burning and consequently that the temperature, size, and mass of the firebrands may change in time. Figure 2 presents a schematic of the coordinate system used and the forces considered in the formulation of the problem.

Assuming that the firebrand mass ablates uniformly from its surface so that net forces due to mass change sum to zero, and that the firebrand density is large compared to the surrounding atmosphere so that buoyancy forces may be neglected, the Newtonian equations of motion for a firebrand in vector form are [15]:

$$\ddot{\vec{x}}_{\mathrm{p}} = F_D \frac{\vec{v}_p - \vec{v}_W}{\left\| \vec{v}_p - \vec{v}_W \right\|} + m_p \vec{g} \tag{14}$$

$$\vec{v}_p = \dot{\vec{x}}_{\mathrm{p}} = \frac{d\vec{x}_p}{dt} \tag{15}$$

where $\vec{v}_p$ is the velocity of the firebrand with respect to the ground, $\vec{x}_p$ is its position relative to the coordinate origin, and $\vec{g}$ is the gravity acceleration. The drag force is:

$$\vec{\mathbf{F}}_{Drag} = \frac{1}{2} C_D \rho_{air} A_{proj} \left|\vec{\mathbf{V}}_R\right|^2 \frac{\vec{\mathbf{V}}_R}{\left|\vec{\mathbf{V}}_R\right|} \tag{16}$$

where the relative velocity between the firebrand and the wind is $\vec{V}_R$. The wind velocity $\vec{v}_W = \left[v_{W,x}, v_{W,y}, v_{W,z}\right]$, while assumed to have only a horizontal component, does possess a vertical distribution, which is dependent on the type of terrain. A_{proj} is the projected area of the firebrand and C_D is the drag coefficient, which is a function of both the Reynolds number and the geometric shape of the firebrands. Fluid properties are taken at atmospheric pressure and average film temperature of the ambient fluid and the firebrand surface temperature. While the bulk flow field is likely turbulent, the turbulent scale is assumed to be much larger than the firebrand size, so that the fluidic forces on the firebrand are considered to be within the laminar regime. The solution to the above equations with the corresponding boundary conditions describes the firebrand trajectory.

Although the problem looks straightforward, there are several issues that complicate its solution [15]. The primary one is the modeling of the firebrand burning process because its diameter d_p and mass m_p are functions of the burning rate and consequently time. The time dependent variation of the firebrand mass and diameter affects the gravity and drag forces and through them the trajectory. The woody material of the firebrand may burn as a gas flame or through a heterogeneous surface combustion reaction (glowing smolder) of the wood. Both forms of combustion are maintained by the heat released by the reaction. However, as the reaction progresses the firebrand will char forming a char layer surrounding the firebrand that grows with time. The char may prevent the transport of heat to its interior preventing the release of pyrolyzates and the formation of the gas flame limiting the combustion to the glowing surface reaction. It also may hinder the diffusion of oxygen to its interior preventing further burning of the firebrand. In addition, if there is a relative velocity between the firebrand and the wind, the char layer may be stripped by shear forces which would enhance the smolder reaction of the firebrand. Furthermore, either flaming or smoldering can be hindered if the firebrand is in the fire plume where oxygen concentrations are low. Modeling of these burning processes is difficult and complicates the accurate prediction of the firebrand trajectory. An approach is to use experimental data to develop empirical correlations of the variation with time of the firebrand diameter and mass as it was done in [68,73,79], where the experiments of Tarifa *et al.* [54,62] were used to develop an effective regression rate equation for spherical firebrands by fitting the data with a diameter to the fourth power law:

$$\frac{d\left(D_p^4\right)}{dt} = -2\sqrt{3}\theta^2 t \tag{17}$$

where the burning constant Θ is obtained fitting to the data in [54]. Following a similar approach Anthenien *et al.* [79] developed burning rate expressions for cylinders (twigs) and very thin disks (leaves). Although these studies provide a first step in the modelling of firebrand burning, there is still a need for a more accurate firebrand burning characterization

that would provide information about the transient effects in the burning process and surface temperature as char builds-up, the effect of the type of wood on the burning rate, and so on.

A characteristic example of a firebrand trajectory is given in Figure 9 for cylinders in a buoyant plume from a 40MW fire in a 48 km/hr crosswind [79]. Simulation results for charring cylinders with extinction by a char layer and burnout with no char formed are shown in the figure. It is seen that large firebrands land on the ground closer to their initiation location, and that small firebrands may burn before landing. Simulations by Sardoy *et al.* [73, 74] included both a flaming and smoldering combustion model, which resulted in a similar dual-distribution of firebrands. Larger, flaming firebrands land near the fire front, and a wider distribution of smaller, smoldering firebrands land further downstream [73–74]. Simulations by Kortas *et al.* [75] have also been used to characterize the mass and spatial distributions of firebrands lofted in an experimental wind tunnel from the firebrand generator known as the NIST Dragon [80].

More recent studies by Tohidi *et al.* have mostly investigated *non-combusting* brands both experimentally [81] and numerically [82–83], examining their transport through a three-dimensional wind field generated by a highly resolved CFD simulation. Their probabilistic approach to the problem is a useful framework, and through their adoption of Richards [84] fully deterministic, 3D 6 degree-of-freedom model, the rotation of rod-like firebrands is incorporated and examined using Monte-Carlo studies. Eventual transport of firebrands is shown to be sensitive to the initial conditions of the firebrand, especially the height from which they are released, concluding that lofting and downwind transport cannot be decoupled. This is an issue as generation algorithms are not yet well established and heights are not included. Rotation of the elements in the air was also deemed an important consideration. A recent experimental study by Song *et al.* [61] studied a somewhat similar configuration with smoldering disc-shaped firebrands. Their results showed a bimodal distribution of landing, similar to Sardoy *et al.* [73–74], and developed correlations for this local landing distance.

A less cited approach was to calculate the concentration distribution of aerosols under the assumption that firebrands may be considered as pollutants (aerosols) [76]. Adapting Sutton’s equation on aerosol distributions, the concentration distribution was obtained on the ground level. This approach does not consider the firebrand size, or combustion of firebrands. Kamei investigated urban fires by considering the number of spot fires and their distance from fire origination. Two ranges of wind speeds were considered; less than 15.0 m/s or 54 km/h (group A) or above 15.0 m/s or 54 km/h (group B). With wind speed higher than 15.0 m/s, most of the spot fires are observed within 100 m from the fire source. The number of spot fires decreases as the distance increases. If the wind speed was less than 15.0 m/s, namely, 6.0 m/s (or 22 km/h) to 15.0 m/s, most of the spot fires were observed from 100 m to 600 m from the fire source [77].

An enhanced scenario for firebrand generation may occur within fire whirls, whose strong circulation induces larger radial and vertical velocities that could enhance both fracture and lofting of firebrands [85]. Muraszew *et al.* [64] analyzed the trajectory of firebrands lofted within a fire whirl and performed some preliminary experiments, showing potential

enhancement in vertical lofting. Still, further research is needed on the topic, including the effects of higher fire intensities and velocities on the generation of additional material and further study of potential lofting distances.

A connecting element between transport of firebrands and ignition of a fuel bed is deposition of the firebrands onto a fuel bed. While there are numerous studies which look at whether firebrands generated from a fire can travel a specific distance, the connection between this distance and how these land and attach to a surface has not yet been modeled in detail. Experiments have shown locations where firebrands are often deposited, especially in controlled studies, such as those with the NIST Dragon [13], however more detailed physical insight will be required before this problem can be completely modeled.

5. Detailed review on Current Knowledge for Ignition Induced by Firebrands

5.1 Ignition of Wildland Fuels

Ignition induced by firebrands, similar to firebrand generation, is much less understood as compared to firebrand transport processes. Wildland fuels have a morphology that is very different from that of a continuous solid. Typically, surface fuels consist of fine, solid pieces of biomass, arranged to form a heterogenous porous material. The morphology of the fuel could vary from a powder and very thin pieces (e.g. duff, grass, etc.), to relatively large pieces of woody material (e.g. needles, twigs and branches). The state of the fuel can also change, from moist to dry and live to dead. Consequently, the ignition characteristics of these fuels is complex and presents challenges. Furthermore, the porous character of surface fuels allows for the direct onset of smoldering ignition. Thus, the ignition of these fuels is a highly complex process that depends on the size and state of the firebrand (smoldering/glowing, flaming), characteristics of the fuel bed on which it lands (temperature, density, porosity, moisture content), and environmental conditions (temperature, humidity, wind velocity).

In the ignition of wildland fuels, fine fuels such as grass, leaves, needles, mulch, and compost are typically the easiest and most common type of fuel ignited by firebrands. The large void fraction of these fuels allows the top layer to ignite and burn with sufficient oxygen availability, while thermally insulating the bottom of the burning layer due to the low thermal conductivity of the biomass and air. Because of the low thermal conductivity, the fuel beds have large Biot numbers, ($Bi > 0.1$), and they would be considered to be thermally thick following the definition that the heated layer would be smaller than the fuel thickness. However, on a hot day, when heated by the air or solar radiation, only a relatively thin outer layer of the fuel would be heated up, and the fuel would behave as a thin fuel in some aspects of the thermal problem. The fuels in this layer would reach their pyrolysis temperature much faster than if they were nonporous, while the rest of the fuel underneath the layer would heat up more slowly. Thus, although the wildland fuel bed would, theoretically, be thermally thick, in practice it would behave as thermally thin ($Bi < 0.1$), in the sense that only a thin surface layer of the fuel bed would heat up. How fast it would heat up would depend on the heating source and the morphological characteristics of the fuel bed.

In addition to the complexity that the fuel bed morphology brings, wildland fuels contain moisture, so the heating and evaporation of the moisture complicates the ignition induced by firebrand processes further. This moisture is primarily water, especially in the case of dead biomass fuels, although recent studies have shown that the drying behavior can be more complex with live fuels [1].

5.2 Ignition of Structural Fuels

In WUI fires, urban fires and informal settlement fires, manmade structures can also be ignited by firebrands. The development of the NIST firebrand generators has led to advancement in this topical area [13]. A review by Hakes *et al.* [41] provides an overview of several components of structures that have been identified as vulnerabilities from firebrand spotting; the review highlights insights obtained from the USA [13]. A review by Suzuki [16] describes studies on vulnerabilities related to Japanese construction in urban fires. Specifically mentioned are: roofing, gutters, eaves, vents, siding, windows, glazing, decks, porches, patios, fences, mulches and debris. These vulnerable components themselves can serve as the fuel itself, but they can serve as a place for fine fuels to collect, such as leaf or pine litter from nearby trees. These fine fuels tend to collect in crevices along the structures, such as areas of roofs, patios, decks, and gutters, easily igniting once firebrands land on a dry windy day. These building features can also provide a path for firebrands to enter the interior of the home, e.g. vents and open windows. Thus, the fuels that can be ignited by firebrands in structures are much more diverse than natural wildland fuels, encompassing synthetic fuels used in roofing or siding and minimally-processed biomass-derived fuels such as decking. These fuels also span the range from very fine fuels (pine and leaf litter) to larger wood components (decking). Large wood components have low porosity (small void fraction) and typically require more heat to ignite. Consequently, these larger materials require more significant flame interactions and/or accumulation of firebrands to overcome the demand imposed by the larger energy requirements.

5.3 Individual Ignition Induced by Firebrands - Studies in the Laboratory

Several studies have examined the ability of single or multiple firebrands to ignite fuels while changing parameters related to the firebrand, fuel, and ambient conditions. Manzello and co-workers [86–89] studied the ability of firebrands, in either a flaming or glowing state, to ignite vegetative fuel beds (pine straw, hardwood mulch, and cut grass) at two moisture content (MC) values and two wind speed levels [86–87]. It was found that although possible, it is unlikely for glowing firebrands to ignite the fuels tested even when they were very dry [86–87]. Flaming firebrands were capable of igniting the finer fuels, when the fuel had a MC of 11%, but ignition was not observed for hardwood mulch and observed half of the time for the cut grass [87]. Similar experiments were done for the spot ignition of crevices in various wood-based construction materials [89].

One aspect of the ignition of a fuel bed by firebrands that has not been studied much is the potential of a smolder ignition of the fuel bed instead of a flaming ignition. It is possible for firebrands to ignite a smolder that would propagate and eventually transition into flaming. This is actually a very likely mode of ignition by glowing firebrands if the fuel and ambient conditions are appropriate. Furthermore, the limiting conditions for ignition are different for

smolder than for flaming. In a related work, Urban *et al.* [90] studied the ignition propensity of low moisture crashed dry grass by hot steel particles and showed that smolder ignition could be achieved at lower particle temperatures and sizes than flaming ignition. Although this indicates that smolder ignition is easier to achieve in terms of the energy requirements of the firebrand, the low intensity of the smolder reaction makes it very sensitive to heat loses to the surrounding fuel and ambient, and consequently more difficult to self-sustain than a flaming fire. This, together with the narrow conditions that cause the transition from smolder to flaming make these type of studies difficult to conduct.

In work at the National Research Institute of Fire and Disaster (NRIFD) in Japan [91], firebrands were produced by igniting wood cubes (Japanese Cypress) using a hot plate (500 °C degrees) and then extinguishing the flame, keeping them in glowing state. The reason to use a hot plate was to provide consistent initial heating to the cubes. Firebrands were deposited on fuel beds placed in front of the fan. Five different sizes of firebrands, 5 mm, 8 mm, 12 mm, 15 mm, and 30 mm were used for this experimental series. The fuel beds were leaves of Japanese Larch, Sawtooth Oak, and Japanese cedar. The influence of wind speed, MC, and fuel bed density was investigated. The MC as well as the wind speed had effect on the minimum firebrand size which could cause ignition under the same density. The degree of the effects depended on the fuel beds, Japanese Larch being the easiest to be ignited.

In another study by Hayashi [92], after the 3-story wooden school burn experiment, it was observed that firebrands caused ignitions on bamboo leaves so experiments with bamboo leaves were performed. 1 cm or 2 cm wood cubes were heated in a cone calorimeter and placed on or in the bamboo leaves. The MC of bamboo leaves was also changed, and two wind speeds, no wind and 1 m/s wind, were tested to investigate the ignition as well as flame spreads. With no wind applied it was difficult to ignite fuel beds with 4.3 % MC with 1 cm cubic firebrands, and with wind applied ignition was observed. When firebrands were placed on top the fuel bed with wind, ignition was observed at MC up to 60 %, but no flame spread. When firebrands are placed inside the fuel beds, ignition was observed at MC 80 %, and flame spread was observed up to 35 % MC.

Additional laboratory experiments have been also conducted attempting to understand the basic mechanisms of the ignition of natural fuel beds by firebrands [93–94]. In those experiments wooden cylinders of different sizes were ignited to flaming or glowing and dropped on a fuel bed of cellulose or saw dust to observe the necessary conditions for a firebrand to ignite a propagating smolder or flaming fire. The work resulted primarily in qualitative information about the smoldering or flaming ignition of cellulose fuel beds. In an extension of that work Urban *et al.* [95] conducted experiments on the effect of the MC of the fuel on the smoldering ignition of sawdust by firebrands. The MC limiting boundary, which for a given size firebrand represents a 50% chance of smoldering ignition of the sawdust, was determined by performing a logistic regression on the experimental results. They show that larger firebrands are capable of igniting sawdust with MC up to 40%, although with very low probability, which is reasonable since they have a larger energy content to evaporate the water contained in the fuel. When the firebrand is sufficiently large (> 9.5 mm), the dominant process governing ignition is whether the target fuel’s combustion releases more heat than the energy required to dry the water in the fuel and raise the

temperature of the fuel to the temperature at which smoldering reactions will occur. The MC ignition boundary then decreased as the firebrand size decreased. It was found firebrands smaller than 4 mm were unable to ignite a fuel smolder with a moisture content below 1%.

An important parameter controlling spot fire ignition by firebrands in all of these studies was the MC of the fuel bed. The importance resides in the fact that the firebrand must evaporate the water in the fuel before the fuel can be ignited by the firebrand, and consequently must have enough energy to first evaporate the water, and subsequently pyrolyze the fuel and ignite the pyrolyzate [96]. The fuel moisture content also affects the net heat released from vegetative fuels, and consequently the sustainment of the fuel bed burning. [97]. Statistical experiments of the effect of MC on the likelihood of smoldering ignition of wildland fuels has been used to evaluate the ignition hazard of wildland fuels by firebrands of several sizes [98].

Recent work by Hakes *et al.* [99] isolated heating from piles of cylindrical firebrands, comparing ignition over real fuels to heat fluxes received by inert, instrumented surface. Tests over an inert sensor array showed that peak and total heating increased with the mass of a deposited pile of firebrands; however, these were not sensitive to diameter and tended to plateau at higher masses, although a larger area was heated. A comparison of ambient tests, which reached a peak heat flux of ~10 kW/m^2, showed a dramatic difference with tests when a 1.84 m/s wind applied, where heat fluxes peaked over 25 kW/m^2, although tests with the same mass of firebrands decreased in heating duration due to faster burnout of firebrands. Further quantitative study with wind was recommended, especially understanding the mechanisms of heating, namely the proportion of radiation vs. conduction and contact.

5.4 Ignition Theories

Very few analytical or modeling studies have been conducted on the ignition of wildland or structural fuels by firebrands or by hot particles. One challenge necessary to model ignition from firebrands is characterization of the transition between smoldering combustion to flaming combustion when fuels are ignited by glowing firebrands. More work has been conducted related to ignition theories for hot non-reacting particles. While this is a far simpler problem than ignition induced by firebrands, these theories are reviewed here for completeness. It has been suggested that the energy content of a particle can be used as an ignition criterion, analogous to the minimum ignition energy concept for gases. Essentially, if the energy content of a particle is greater than a particular threshold, then ignition occurs. However, this criterion is insufficient because it has been shown experimentally that different size particles with the same energy do not necessarily result in ignition [15]. On the other hand, the “hot spot” ignition theory [100–101] appears to provide a reasonable and simple approach for the prediction of particle size-temperature relationships for ignition. Hot spot theory was originally developed to model the ignition of gases by hot particles [100–101] and the ignition of a condense explosives [102]. Later on Jones [103–105] applied hot spot theory developed by Gol’dshleger *et al.* [102] to simulate the ignition of forest litter by copper particles. The application of this theory was also recommended by Bowes [106] for its compromise between accuracy and tractability and was also applied by Babrauskas [29] to correlate barley grass ignition by aluminum particles [107]. Hadden *et al.* [108] applied

the hot spot theory to correlate their experiments on the ignition of a cellulose fuel bed by hot steel particles and found that although the theory was in qualitatively agreement with the experimental observations it was not capable of providing quantitative results. Several recent studies have also been conducted that are critical to advance understanding of hot metal particle ignition [109–111]. Here we describe briefly the theory since it has a potential application to the prediction of wildland fuel ignition by firebrands.

The governing equations for a non-reactive hot spot particle/firebrand (subscript p) completely embedded in an infinite fuel bed are as follows:

$$\text{for} 0 < \mathrm{x} < r: \qquad \rho_p c_p \frac{dT_p}{dt} = \frac{a_p}{V_p} k \nabla T \Big|_{x = r^+} \tag{18}$$

$$\text{for} r \leq x < \infty: \qquad \rho c_p \frac{\partial T}{\partial T} = \nabla \cdot k \nabla T + \rho A \Delta H \exp\left(-\frac{E}{RT}\right) \tag{19}$$

where ρ is the density, c_p is the specific heat capacity, T is the temperature, t is time, a is the surface area, V is the volume, k is the thermal conductivity, A is the pre-exponential factor, ΔH is the heat of combustion, E is the activation energy, and R is the universal gas constant.

In formulating the energy equation for the particle, Eq. (18), it has been assumed that the particle temperature is uniform and that the particle is in good thermal contact with the surrounding fuel bed so that the rate of heat transfer from the particle is $a_p k \nabla T$ where a_p is the particle surface area.

The initial conditions for Eq. (18) are:

$$\text{for} 0 < x < r \quad T_p\big|_{t=0} = T_{p0} \quad \text{and for} r \leq x < \infty \quad T\big|_{t=0} = T_0$$

and for Eq. (19):

$$T\big|_{x \to \infty} = T_0 \quad \text{and} \quad T\big|_{x = r^+} = T_p$$

Equations (18) and (19) cannot be solved analytically and require numerical solution. Of primary interest is the value of the particle radius at which thermal runaway (ignition) occurs. Gol'dshleger *et al.* [102] conducted numerical simulations to determine the value of the critical radius for ignition (δ_{cr}) and found that the following curve-fit matched their numerical results within 10%:

$$\delta_{cr} \approx 0.4\sqrt{b^2 + 0.25n(n+1)\left(b + 0.1b^3\right)}(2.25(n-1) - \theta_0)^2(1 - 0.5\beta\theta_0) \tag{20}$$

where δ_{cr} is the Frank-Kamenetskii hot spot parameter; b the volumetric heat capacity ratio; and β,, the dimensionless inverse particle temperature are defined as follows:

$$\delta = r\sqrt{\frac{\rho A \Delta H}{k}\frac{E}{RT_{p0}^2}\exp\left(-\frac{E}{RT_{p0}}\right)} \tag{21}$$

$$b = \frac{\rho c}{\rho_p c_p} \tag{22}$$

$$\beta = \frac{RT_{p0}}{E} \tag{23}$$

Once δ_{cr} is calculated from Eq. (20) the critical hot spot radius r_{cr} (*i.e.*, the minimum particle radius for ignition) can be calculated from the definition of δ (Eq. 21) as:

$$r_{cr} = \delta_{cr}\sqrt{\frac{k}{\rho A \Delta H}\frac{RT_{p0}^2}{E}\exp\left(\frac{E}{RT_{p0}}\right)} \tag{24}$$

Eq. (24) predicts qualitatively the experimental observations of [107–108] that the critical particle size for ignition of a natural fuel bed increases as the temperature of the particle decreases.

Given the simplified character of the hot spot theory several numerical models of differing degree of accuracy have been developed to simulate more accurately the ignition of a wildland fuel bed by a hot particle or firebrand. Zvyagils'kaya and Subbotin [112], Grishin *et al.* [113], and Matvienko *et al.* [114] developed numerical models that considered a porous condensed-phase that represented natural vegetation. However, the models do not include a porous condensed-phase model (to simulate the fuel bed) coupled to a gas-phase code (to simulate the exterior "ambient"). This coupled approach is required to properly simulate the ignition mechanisms of a fuel bed by a firebrand. To provide a more accurate insight into the spot fire ignition problem Lautenberger and Fernandez-Pello [115] developed a 2-D coupled gas/solid analysis of the ignition induced by a firebrand. The model consists of a computational fluid dynamics representation of the gas-phase using Fire Dynamic Simulations (FDS) [116] coupled to a heat transfer and pyrolysis model, G-Pyro [117] that simulates condensed-phase phenomena. The coupled model is used to simulate ignition of a powdered cellulose porous fuel bed by glowing firebrands made from pine in a laboratory experiment. The model provides qualitative information regarding the mechanisms leading to ignition, smolder, or flame propagation on porous fuel bed that agree qualitatively with experimental observations. The model provides the foundation for a more complete study of the problem where the effects of different factors (moisture content, humidity, temperature, porosity, particle size/heat content, etc.) are quantified. Another notable numerical model of the ignition induced by firebrand problem is that of Matvienko *et al* [114]. The model is a 3-D numerical model that considers the exchange of heat between the fuel bed and the surrounding air, and the evaporation of moisture from the fuel. The objective of the model is to determine the temperatures and concentration of components for fuel-bed and gas-phase ignition. The model predictions for the limiting conditions for ignition agree well with experiments conducted to verify the model.

Yin *et al.* [118] formulated a scaling analysis based on a simple thermal conservation equation, proposing a correlation between the ignition time of a loose vegetative fuel bed:

$$\sqrt{t_{ig}} \sim \frac{q\sqrt{(\rho_F k)/c_p}}{(\rho Z \Delta H_C)/t_b - h_T(T_F - T_0)} \tag{25}$$

where t_{ig} is the time to ignition after firebrand deposition, q is the heat required for ignition of moist fuel on a dry-mass basis, ρ_F the initial density of the firebrand, k, ρ, and c_p the thermal conductivity, density and specific heat of dry pine needles in the bed, respectively, Z the height of the firebrand, ΔH_c the heat of combustion of the firebrand in a glowing phase of combustion, h_T the heat loss coefficient, T_F the firebrand temperature, and T_0 the initial temperature of the target fuel bed [118]. A linear relationship is seen between $\sqrt{t_{ig}}$ and q, which corresponds with the slope observed in experiments on Chinese lodge pole pine [119–120]; however, the comparison is not quantitative.

5.5 Experimentally Simulating Firebrand Showers

A major challenge related to firebrand transport and ignition understanding is related to the *showers* of firebrands that are generated in actual large outdoor fires. While studying the fundamental ignition processes of individual firebrands is important, these studies are not able to quantify the vulnerabilities of structures to ignition from firebrand showers or elucidate the physics of firebrand transport. To accomplish this requires measurement methods that are capable to replicate wind-driven firebrand showers that occur in actual large outdoor fire events. To address this problem, the NIST Firebrand Generator was constructed to generate controlled, repeatable firebrand showers commensurate to those measured from actual large outdoor fires [80] and then modified to produce the firebrand showers for continuous duration (see Figure 10).

Both full-scale [121] and reduced-scale versions [122] of this experimental technology have been developed that are able to produce a continuous flow of firebrand showers. For completeness, the principles of operation for the full-scale continuous feed firebrand generator is described and the principles of operation are similar for the reduced-scale version of the apparatus.

The experimental apparatus consists of the main body and the continuous feeding component (Dragon component). In this experimental apparatus, airflow required for firebrand combustion/lofting was provided by a variable frequency drive blower that was coupled to the main body. The airflow speed was initially varied to determine optimal operating conditions for glowing firebrand generation. The purpose of the experimental apparatus is to simulate wind-driven firebrand showers observed in long-range spotting. As a result, glowing firebrands were the initial emphasis. Yet, due to careful design of the device, it is also possible to generate showers of flaming firebrands.

The feeding system made use of a large air driven cylinder. A custom constructed receptacle was used to store the wood chips. Directly beneath the wood storage area, a custom metal plate was fitted that allowed changes in the volume of wood to fall from the storage receptacle to the first gate. By adjusting this volume, the amount of wood chips that enter the

main body (Dragon) for eventual combustion could be varied. When the air pressure was energized, the rod of the air cylinder slid forward and separated the wood pieces from the storage receptacle to the first gate, where they were then deposited towards the second gate that led to the Dragon where they were ignited using a propane fueled burner that was kept on continuously during the experiments. Since wind is an important component of large outdoor fire spread, the full-scale version of the NIST Dragon is installed inside the BRI's FRWTF.

The reduced-scale continuous feed firebrand generator is installed inside the NRIFD's wind facility. The flow field is much smaller than the BRI facility at 2 m by 2m, so it is possible to conduct smaller scale experiments to observe the physics of firebrand transport and ignition. Differences in the full-scale behavior may be directly compared using this smaller sized facility.

These collaborative efforts between NIST, BRI, and NRIFD have led to advances in the understanding of firebrand process in large outdoor fires. As some examples, Figure 11 demonstrates how the full-scale firebrand generator may be used to investigate firebrand flow over obstacles on realistic-scales. Wind-driven showers of firebrands have been used to investigate the ignition of whole building components, such as ceramic roofing assemblies [123–132]. This is an important aspect of the ignition problem, as accumulated `piles' of firebrands store significantly more energy, posing a much greater ignition hazard. In addition of studying the effect of basic parameters, such as the characteristics of the firebrand and fuel bed, in the propensity of the firebrand to ignite the target fuel, these studies address realistic scenarios such as the ignition of fences and decks by accumulation of firebrands. These works confirmed that firebrand showers and the accumulation of firebrands in deck crevices, fence corners, vertical walls and garden mulch, enhances the ability of the firebrands to ignite structures. Manzello and co-workers [123–132] also studied the attack of siding and building components to firebrand showers and investigated the vulnerabilities of the different components. An interesting finding is that firebrand showers can ignite mulch in re-entrant corners like those found in homes which in turn can ignite the siding.

Recent experiments have used the reduced-scale continuous feed firebrand generator to unravel the basic ignition dynamics of thatched roofing assemblies [132]. While it has been known that important cultural heritage sites that contain thatched roofing assemblies are prone to ignition, it has not been possible to experimentally explore the fundamental ignition mechanisms. In Figure 12, a mock-up thatched roofing assembly is exposed to firebrand showers characteristic of those produced from structure combustion using the reduced-scale firebrand generator in NRIFD. These experiments are useful to evaluate and develop effective counter measures to protect historical structures with thatched roofing assemblies, especially for historical buildings, such as the United Nations Educational, Scientific and Cultural Organization (UNESCO)'s world heritage sites in Japan.

6. Research Needs

Experiments, models, and simulations related to firebrand generation, lofting, burning, transport, deposition and ignition of materials were reviewed in the context of large outdoor

fires. Over the past several decades, the fire safety science discipline has developed a deep body of knowledge on fire dynamics within buildings [133]. As opposed to traditional building fires, there exists no validated models to predict fire spread and structure ignition in large outdoor fires. As a result, the importance of firebrand processes is listed as a major global research focus by the International FORUM of Fire Research Directors [133]. While extensive progress has been made in firebrand research, some key areas that require further attention are delineated with an emphasis on areas where the *fundamental combustion research community* may play a leading role.

Well-controlled experiments on firebrand transport and deposition under applied wind fields and different fuel bed morphologies are required. Basic understanding is required on how firebrands may deposit in the presence of various obstacles under wind.

New experimental methodologies, based on state of the art imaging techniques, to characterize the firebrand flux from actual fire sources, from various building elements, and vegetative fuel sources. The ability to actually measure firebrand fluxes and firebrand temperatures from various fuel sources is needed.

To be able to better describe firebrand combustion process, improved transient models of firebrand burning (flaming and glowing) including char growth, effect of the char layer on a firebrand's burning rate, and extinction by the growth of a char layer are needed.

More experimental ignition data from structural fuel elements, especially with a focus small crevices and grooves. Firebrands are known to be able to ignite decking assemblies and other construction features due their ability to become lodged into gaps and crevices. More experimental work is needed to better quantify these ignition events.

Better experimental methodologies and associated models to characterize firebrand generation from real fire sources, such as actual WUI, urban, and informal settlement fires. To be able to improve firebrand generation models requires much needed experimental data. At the same time, firebrand generation experiments require improved measurement methods to characterize effective fire size coupled to the firebrand generation data.

Understanding of the combined effects of firebrands and radiant or convective heat on ignition of diverse fuels. Nearly all the past research has been limited to only ignition induced purely by firebrand contact. Yet, it is natural to assume coupled influences of radiant, or convective, heat from surrounding fire sources may only ease ignition of fuels exposed to firebrand showers.

To be able to provide for better community resilience to large outdoor fire exposures to firebrand showers requires internationally accepted test standards. To this end, a globally accepted testing methodology to evaluate material performance and structure design for firebrand exposures is needed.

7. Summary

Large outdoor fires represent an increasing problem of global importance. A commonality in the rapid spread of large outdoor fires, such as WUI fires, urban fires, and informal settlement fires, are the production or generation of new, far smaller combustible fragments from the original fire source referred to as firebrands. In the most simplistic representation, firebrand processes may be divided into several sub-processes, namely the generation of firebrands, their transport by plume lofting and drag forces with the wind, thermo-chemical degradation during flight, deposition onto and ignition of fuel beds by either flaming or smoldering, and the subsequent surface spread of the fire. The current state of the art on these topics was reviewed, highlighting some recent progress. Yet, numerous other issues are needed in this complex process.

The generation of firebrands remains one of the least understood sub-processes. While recent studies have started to look at the mechanisms that generate firebrands, none have yet been adapted into a numerical formulation capable of initializing firebrand generation, in terms of mass, number, and so on, within numerical models. Future simulations necessitate a means to initialize firebrands from specific fuels under different burning and wind conditions so that past or future fire events can be simulated. The distribution of firebrands coming off certain burning items under wind, mostly vegetation and structural components, has started to be well-detailed more recently, including distributions of size and mass of firebrands. Once models are developed, a host of validation exercises is possible.

The transport, lofting and thermal degradation of firebrands has been relatively well described compared to other processes. Starting with simplified models for the maximum distance firebrands can fly, followed by coupled thermo-fluid lofting formulations, there are a variety of well-described approaches in the literature already adapted into numerical codes that describe the transport of firebrands both for simple 2-D surface spread calculations and 3D CFD simulations. While future development is still possible in this area, including issues such as the influence of initial location of the firebrand, effects of rotation in transport, further study of firebrand thermal degradation, and so on, the lack of an ability to initialize firebrands in the first place shifts the priority to other aspects of the problem.

The deposition of firebrands and their eventual ignition of smolder or flaming vegetative spot fires or structure ignition remains a critical, underserved area of study. Deposition is incredibly underserved and mostly appears only in coupled experiments with a firebrand generator under wind. These experiments are important as they identify critical vulnerabilities in different structural components, leading to changes in vent, eave, and other designs and test standards that enhance public safety. Still, fundamental experiments capable of describing the locations where firebrands will deposit or critical conditions for ignition based on some form of firebrand deposition properties are few and quite limited. Several studies have identified critical conditions for ignition of vegetative fuels and less for structural materials, but a theory or formulation that is more universal in nature, going beyond the experimental conditions, is lacking. This is important for future model development, which may rely on a probabilistic basis of ignition induced by firebrand, incorporating the even more complex process of transition from smoldering to flaming.

Identifying key thermal parameters at ignition, rather than just the ignition thresholds, may help to inform the development of these futures models, as well as improved modelling of both firebrand degradation/heating and eventual ignition of materials using state-of-the-art solid-phase models which already exist in the field. The authors hope future research will continue to unravel this complex problem in an effort to better mitigate the destruction from large outdoor fires.

Acknowledgements

SS would like to acknowledge Dr. Shinohara of NRIFD for providing data from the Beppu-city fire. SS also would like to acknowledge Dr. El Houssami of Plastics Europe for providing data from a prescribed burn in 2013. CFP would to acknowledge Dr. J. Urban for assistance preparing the manuscript.

9. References

1. Manzello SL, Blanchi, R. Gollner MJ, Gorham D, McAllister S, Pastor E, Planas E, Reszka P, and Suzuki S, Fire Safety J. 100: 76–92 (2018).
2. Manzello SL, Summary of Workshop on Global Overview of Large Outdoor Fire Standards, NIST Special Publication 1235 (2019).
3. Japan Association for Fire Safety Engineering, (2018) Kasai Binran: Handbook for Fire Science and Engineering, 4th Edition, Kyoritsu
4. Krieger. LM Wine Country Fires: Why are they so deadly, destructive, and difficult to stop? (2017).
5. Top 20 Most Destructive California Wildfires. CALFIRE (2017)
6. California Statewide Fire Summary. CALFIRE (2017)
7. Thomas Fire Incident Information. CALFIRE (2018).
8. Mielke B and Hutchinson B: This was a firestorm: Deadly California wildfire leaves entire Paradise town council homeless. ABC News, 2018.
9. City of Hakodate; Hakodate Taika (the 1934 Hakodate Fire).
10. Suzuki S, and Manzello SL, Characteristics of Firebrands Collected from Actual Urban Fires, Fire Techn. 54, 1533:1546 (2018).
11. Pastor E, Zarate L, Planas E, and Arnaldos J, “Mathematical models and calculation systems for the study of wildland fire behaviour,” Prog. Energy Combust. Sci, vol. 29, pp. 139–153, 2003.
12. Koo E, Pagni PJ, Weise DR, and Woycheese JP, “Firebrands and spotting ignition in large-scale fires,” Int. J. Wildl. Fire, p. 818, 2010.
13. Manzello SL, Enabling the Investigation of Structure Vulnerablities to Wind Driven Firebrand Showers, Fire Safety Science 11: 83–96 (2014).
14. Caton SE, Hakes RSP, Gorham DJ, Zhou A, and Gollner MJ, “A Review of Pathways for Building Fire Spread in the Wildland Urban Interface Part I: Exposure Conditions,” Fire Technol, vol. 53, no. 2, pp. 429–473, 3 2017.
15. Fernandez-Pello AC, “Wildland fire spot ignition by sparks and firebrands,” Fire Saf. J, vol. 91, 2017.
16. Suzuki S, ‘A Review on Structure Ignitions by Firebrands’, Bulletin Of Japan Association For Fire Science And Engineering, Vol. 67, No. 1 (2017) pp.49–55. (in Japanese)
17. Manzello SL, Maranghides A, and Mell W, “Firebrands Generation from Burning Vegetation” Int. J. Wildland Fire, 16, 458–462 (2007)
18. Wischkaemper JA, Benner CI and Russell BD ”Electrical Characterization of Vegetation Contacts with DistributionConductors – Investigation of Progress Faults Behavior “ Proc. of the PES T&D Conf. & Expo, Chicago, Il (2008)
19. National Research Institute of Fire and Disaster, Fire Spread Behaviors of The Sakata Fire, Technical Report of National Research Institute of Fire and Disaster, No.11, 1977 (in Japanese).
20. Pagni PJ “Cause of the 20 October 1991 Oakland Hills conflagration” Fire Safety Journal 21, 331–339 (1993)

21. Ohmiya Y and Iwami T, An Investigation on the Distribution of Firebrands and Spot Fires due to a Hotel Fire, Fire Sci Technol. 20 (2000) 27–35.
22. Manzello SL, Foote EID, Characterizing Firebrand Exposure During Wildland-Urban Interface Fires: Results of the 2007 Angora Fire, Fire Technol. 50 (2014) 105–124.
23. Rissel S, and Ridenour K., Ember Production During the Bastrop Complex Fire, Fire Management Today, 72: 7–13 (2013).
24. Shinohara M, Sugii K, Hosokawa M, The influence of Characteristics of Firebrands on the Flight Distance – Based on the Field Survey of the City Fire under the Strong Wind in Beppu-city, Oita, in January 2010-, Report of National Research Institute of Fire and Disaster, No. 113, Chofu, Tokyo, 2012 (in Japanese).
25. Suzuki S, 'Study on characteristics of firebrands collected from three different fires' Report of National Research Institute of Fire and Disaster, No. 123, pp.1–9. Chofu, Tokyo, 2017 (in Japanese)
26. National Research Institute of Fire and Disaster, Investigation report on 2016' Itoigawa-city Urban fire, Technical Report of National Research Institute of Fire and Disaster, No.84, 2018 (in Japanese).
27. Holmes J, Baker C, Tamura Y, Tachikawa Number, A Proposal, J. Wind. Ind. Eng. Aerodyn 94: 41–47 (2006).
28. Hayashi Y, Jaishi T, Izumi J, Naruse T, Itagaki N, Hashimoto R, Yasui N, Hasemi Y, Firebrands Deposition and Measurements of Collected Firebrands Generated and Transported from a Full-scale Burn Test using a Large Wooden Building, AIJ J. Techgnol. Des 20 (2014) 605–610 (in Japanese)
29. Babrauskas V, Ignition Handbook: Principles and Applications to Fire Safety Engineering, Fire Investigation, Risk Management, and Forensic Science, Fire Science Publishers, Issaquah, WA, 2003.
30. Tohidi A, Kaye N, and Bridges W, "Statistical description of firebrand size and shape distribution from coniferous trees for use in Metropolis Monte Carlo simulations of firebrand flight distance," Fire Saf. J, vol. 77, pp. 21–35, 2015.
31. Manzello SL, Maranghides A, Shields JR, Mell WE, Hayashi Y, and Nii D, Mass and Size Distribution of Firebrands Generated from Burning Korean Pine (Pinus Koraiensis) Trees, Fire and Materials, 33:21–31, 2009.
32. Mell WE, Maranghides A, McDermott R, and Manzello SL, Numerical Simulation and Experiments of Burning Low-Moisture Douglas-Fir Trees, Combustion and Flame, 156:2023–2041, 2009.
33. Manzello SL, Maranghides A, Mell W, Sheilds JR, Hayashi Y, and Nii D, Measurement of Firebrand Production and HRR (HRR) from Burning Korean Pine Trees, Proc. of 7th Asia-Oceania Symposium on Fire Science and Technology, Hong Kong, China, 2007.
34. National Research Institute of Fire and Disaster, Development of prediction system for likelihood of forest fires and forest fire spreads, Technical Report of National Research Institute of Fire and Disaster, No.63, 2004 (in Japanese).
35. Houssami El, et al., "Experimental procedures characterizing firebrand generation in wildland fires", fire technology, 52(3), 731–751 (2016).
36. Filkov A, Prohanov S, Mueller E, Kasymov, Martynov P, El Houssami M, Thomas J, Skowronski N, Butler B, Gallagher M, Clark K, Mell W, Kremens R, Hadden RM, and Simeoni A"Investigation of Firebrand Production During Prescribed Fires Conducted in a Pine Forest" Proceedings of the Combustion Institute, 36, 3263–3270 (2017)
37. Thomas JC, Mueller EV, Santamaria S, Gallagher M, El Houssami M, Filkov A, Clark K, Skowronski N, Hadden RM, Mell W, Simeoni A, Investigation of Firebrand Generation from an Experimental Fire: Development of a Reliable Data Collection Methodology, Fire Safety Journal 91, 864–871 (2017)
38. Mandelbrot BB (1977) The fractal geometry of nature. W.H. Freeman and Company, New York
39. Collin A, Lamorlette A, Bernardin D, Séro-Guillaume O (2011) Modelling of tree crowns with realistic morphological features: new reconstruction methodology based on iterated function system tool. Ecol Model 222:503–513.

40. Barr BW and Ezekoye O, “Thermo-mechanical modeling of firebrand breakage on a fractal tree,” Proc. Combust. Inst, vol. 34, pp. 2649–2656. 2013.
41. Caton S (2016) Laboratory studies on the generation of firebrands from cylindrical wooden dowels. Masters thesis, University of Maryland, College Park.
42. Hayashi Y, Iwami T, “Development of Urban fire simulator Incorporated with spot fires caused by firebrands” The BRI annual report, pp 89–90. (2010) (in Japanese)
43. Vodvarka FJ, Firebrand Field Studies—Final Report, IIT Research Institute, Chicago, IL, 1969.
44. Vodvarka FJ, Urban Burns-Full-scale Field Studies—Final Report, IIT Research Institute, Chicago, IL, 1970.
45. Waterman 1969 Experimental Study on Firebrand Generation, IIT Research Institute, Chicago, IL.
46. Yoshioka H (2006) Study on urban fire propagation by firebrand generation and transport PhD thesis, The University of Tokyo, Tokyo (in Japanese)
47. Hasemi Y, Yasui N, Itagaki N, Izumi J, Osaka T, Kaku T, Naruse T, Hagiwara I, Kagiya K, Suzuki J, Kato K, Full-scale fire tests of 3-story wooden school building, World Conference on Timber Engineering, Quebec City, Canada, August 2014
48. Suzuki S, Manzello SL, Lage M, Laing G, Firebrand Generation Data Obtained From a Full Scale Structure Burn, Int. J. Wildland Fire 21 (2012) 961–968.
49. Suzuki S, Brown A, Manzello SL, Suzuki J, Hayashi Y, Firebrands Generated from a Full-Scale Structure Burning Under Well-Controlled Laboratory Conditions, Fire Safety Journal, 63 (2014) 43–51.
50. Suzuki S, Manzello SL, Hayashi Y, The Size and Mass Distribution of Firebrands collected from Ignited Building Components Exposed to Wind, Proc. Combust. Inst 34 (2013) 2479–2485.
51. Manzello et al. Quantifying wind-driven firebrand production from roofing assembly combustion, Fire and Materials 43: 3–7,2019
52. Suzuki S, and Manzello SL, ‘Firebrand Production from Building Components Fitted with Siding Treatments’, Fire Safety Journal, Vol. 80 (2016) pp. 64–70. [PubMed: 27114643]
53. Suzuki S and Manzello SL Investigating effect of wind speeds on structural firebrand generation in laboratory scale experiments, International Journal and Heat and Mass Transfer, 130, 135–140 2019
54. Tarifa CS, Notario P, Moreno FG “On the flight paths and lifetimes of burning particles of wood, Proc. Combust, 10 1021 (1965)
55. Baum HR and McCaffrey BJ Fire Induced Flow Field-Theory and Experiments, Fire Safety Science 2: 129–148 (1989)
56. McGrattan KB, Baum HR and Rehn RG “Smoke Plumes from Large Fires” UJNR panel on Fire Research,NIST, Gaithersburgh, MD (1995)
57. Quintiere JG, Grove BS, “A Unified Analysis for Fire Plumes,” Proc. Combust. Inst 27: 2757–2766 (1998).
58. Woycheese JP, Pagni PJ and Liepmann D “Brand Propagation from Large-Scale Fires”, J. Fire Protection Engr. V10, 32–44 (1999)
59. Huang H, Ooka R, Kato S, Otake H, and Hayashi Y CFD Simulation of Thermal Plumes and Firebrands Scattering in Urban Fires, Fire Science and Technology, p. 152–163 (2004)
60. Himoto K, Mauyama T, and Tanaka T, “A study on the brand spotting in urban fires-LES analysis on the scattering of square disks in a turbulent boundary layer,” Proceedings of the 10th Interflam. 1039–1050 (2004).
61. Song J, Huang X, Liu N, Li H, Zhang L The Wind Effect on the Transport and Burning of Firebrands, Fire Technology, 53(4): 1555–1568 (2017)
62. Tarifa CS, Del Notario PP, Moreno FG & Villa AR, Transport and combustion of firebrands U.S. Department of Agriculture Forest Service, Final Report of Grants GF-SP-114 and GF-SP-146. Madrid, (1967).
63. Lee SL, and Hellman JM, “Firebrand Trajectory Study Using an Empirical VelocityDependent Burning Law,” Combustion and Flame 15: 265–274 (1970).
64. Muraszew A, Fedele JB, and Kuby WC, Trajectory of Firebrands in and out of Fire Whirls, Combustion and Flame 30:321–324 (1977).

65. Albini FA Spot Fire Distance from Burning Trees: A Predictive Model GTR-INT-56. USDA Forest Service, 1979.
66. Albini FA, “Potential Spotting Distance from Wind-Driven Surface Fires,” USDA Forest Service Research Paper ZNT-309 (1983).
67. Albini FA, Tranport of Firebrands by Line Thermals, Combustion and Flame, 32:277288 (1983).
68. Tse SD and Fernandez-Pello AC “On the Flight Paths of Metal Particles and Embers Generated by Powerlines in High Winds - A potential Source of Wildland Fires” Fire Safety J. 30, pp. 333–356. (1998)
69. Woycheese JP, Pagni PJ, and Liepman D, Brand Lofting Above Large-Scale Fires, 2nd International Conference on Fire Research and Engineering, Boston, MA, (1998).
70. Himoto K and Tanaka T “Transport of Disk-Shaped Firebrands in a Turbulent Boundary Layer,” Fire Safety Science 8: 433–444 (2005).
71. Koo E, Pagni P, and Linn R, “Using FIRETEC to Describe Firebrand Behavior in Wildfires,” Fire and Materials 2007, San Francisco, CA (2007).
72. Linn R, Resiner J, Colman JJ, and Winterkamp J, “Studying wildfire behavior using FIRETEC,” International Journal of Wildland Fire 11: 233 – 246 (2002).
73. Sardoy N Consalvi J-L, Poterie B, Loraud J-C and Fernandez-Pello CA “Modeling Transport and Combustion of Firebrands from Burning Trees”. Combustion and Flame, V 150, 151–169, (2007)
74. Sardoy N, Consalvi J-L Kais J-L, Poterie B and Fernandez-Pello C “Numerical Study of Ground-level Distribution of Firebrands Generated by Line Fires” Combust. Flame, 154, 478–488 (2008)
75. Kortas S, Mindykowski P, Consalvi JLL, Mhiri H, and Porterie B, “Experimental validation of a numerical model for the transport of firebrands,” Fire Saf. J, vol. 44, pp. 1095–1102, 2009.
76. Japan Association for Fire Safety Engineering, (1955) Kasai Binran: Handbook for Fire Science and Engineering, Rikasyoin.
77. Kamei K, (1959) ‘Taikaji ni okeru fusoku to Tobihi ni kansuru kenkyu’, Transactions of the Architectural Institute of Japan, vol. 62, 115–121.
78. Suzuki S and Manzello SL, Experimental Investigation of Firebrand Accumulation Zones in Front of Obstacles, Fire Safety Journal, 94: 1–7, 2017.
79. Anthenien RA, Tse SD, and Fernandez-Pello C,“On the Trajectories of Embers Initially Elevated or Lofted by Small Scale Ground Fire Plumes in High Winds,” Fire Safety J. 41: 349–363 (2006).
80. Manzello SL et al., “On the development and characterization of a firebrand generator,” Fire Saf. J, vol. 43, pp. 258–268, 2008
81. Tohidi A and Kaye NB, “Comprehensive wind tunnel experiments of lofting and downwind transport of non-combusting rod-like model firebrands during firebrand shower scenarios,” Fire Saf. J, vol. 90, no. December 2016, pp. 95–111, 2017.
82. Tohidi A and Kaye NB, “Stochastic modeling of firebrand shower scenarios,” Fire Saf. J, vol. 91, pp. 91–102, 2017.
83. Tohidi A and Kaye NB, “Aerodynamic characterization of rod-like debris with application to firebrand transport,” J. Wind Eng. Ind. Aerodyn, vol. 168, pp. 297–311, 2017.
84. Richards PJ, “Steady Aerodynamics of Rod and Plate Type Debris.pdf,” in 17th Australian Fluid Mechanics Conference, 2010.
85. Tohidi Ali, Gollner MJ, and Huahua Xiao. “Fire whirls.” Annual Review of Fluid Mechanics 50 (2018): 187–213.
86. Manzello SL, Cleary TG, Shields JR, and Yang JC, On the Ignition of Fuel Beds by Firebrands, Fire and Materialsl, 30:77–87, 2006.
87. Manzello SL, Cleary TG, Shields JR, and Yang JC, Ignition of Vegetation and Mulch by Firebrands in Wildland/Urban Interface (WUI) Fires, Int’l J. Wildland Fire,15:427–431,2006.
88. Manzello SL, Cleary TG, Shields JR, Mell W, and Yang JC, “Experimental Investigation of Firebrands: Generation and Ignition of Fuel Beds,” Fire Safety Journal 43: 226–233 (2008).
89. Manzello SL, Park SH, Cleary TG, Investigation on the ability of glowing firebrands deposited within crevices to ignite common building materials, Fire Safety Journal 44 (2009) 894–900.
90. Urban J, Zak C, Song J, and Fernandez-Pello AC, “Smoldering spot ignition of natural fuels by a hot metal particle,” Proc. Combust. Inst, vol. 36, pp. 3211–3218, 2017.

91. National Research Institute of Fire and Disaster, Research on spot fires in forest fires, Technical report No. 21, 1988 (in Japanese).
92. Hayashi Y 'Ignition of firebrands produced from burning wooden buildings', proceedings of annual symposium of Building Research Institute, page 69–70 (2012) (In Japanese).
93. Fereres S, Lautenberger C and Fernandez-Pello C"Preliminary Study of the Ignition of Vegetation Bed by a Firebrand" Workshop on Mathematical Modeling and Numerical Simulation of Forest Fire Propagation, Vigo, Spain 11 29–30, (2008)
94. Fernandez-Pello AC, Lautenberger C, Rich D, Zak C, Urban J, Hadden R, Scott S and Fereres S "Spot Fire Ignition of Natural Fuel Beds by Hot Metal Particles, Embers and Sparks" Combustion Science and Technology, 187:1–2, 269–295 (2014)
95. Urban JL, Song J, Santamaria S, Fernandez-Pello C "Ignition of a Spot Smolder in a Moist Fuel Bed by a Firebrand". Fire Saf. J, 108, (2019).
96. Urban JL, Fernandez-Pello AC, Ignition, in: Manzello SL (Ed.), Encyclopedia of Wildfires and Wildland-Urban Interface (WUI) Fires, Springer, 2018, pp. 1–9.
97. Babrauskas V, Effective heat of combustion for flaming combustion of conifers, Canadian Journal of Forest Research 36 (2006) 659–663.
98. Schroeder MJ, Ignition Probability, Tech. rep., Forest Service (1969).
99. Hakes RSP, Salehizadeh H, Weston-Dawkes MJ, and Gollner MJ, "Thermal characterization of firebrand piles," Fire Saf. J, 2018
100. Friedman MH, "A Correlation of Impact Sensitivities by Means of the Hot Spot Model," Proceedings of the Combustion Institute 9: 294–302 (1963).
101. Thomas PH, "A Comparison of Some Hot Spot Theories," Proceedings of the Combustion Institute 10: 369–372 (1965).
102. Gol'dshleger UI, Pribytkova KV, and Barzykin VV, "Ignition of a Condensed Explosive by a Hot Object of Finite Dimensions," Fizika Goreniya I Vzryva 9: 119–123 (1973).
103. Jones JC, "Predictive Calculations of the Effect of an Accidental Heat Source on a Bed of Forest Litter," Journal of Fire Sciences 11: 80–86 (1993).
104. Jones JC, "Further Calculations Concerning the Accidental Supply of Heat to a Bed of Forest Material," Journal of Fire Sciences 12: 502–505 (1994).
105. Jones JC, "Improved Calculations Concerning the Ignition of Forest Litter by Hot Particle Ingress," Journal of Fire Sciences 13: 350–356 (1995).
106. Bowes PC, Self Heating: Evaluating and Controlling the Hazards, Elsevier, 1984.
107. Rowntree GWG and Stokes AD, "Fire Ignition by Aluminum Particles of Controlled Size," Journal of Electrical and Electronics Engineering, Australia 14: 117–123 (1994).
108. Hadden R, Scott S, Lautenberger C and Fernandez-Pello C "Ignition of Combustible Fuel Beds by Hot Particles: An Experimental and Theoretical Study" Fire Technology, V47, 341, (2011).
109. Wang S, Chen H, and Liu N, Ignition of Expandable Polystyrene Foam by a Hot Particle: A Numerical and Experimental Study, J. Haz. Materials 283: 536–543 (2015).
110. Wang S, Huang X, Chen H, Liu N, and Rein G. Ignition of Low Density Expandable Polystyrene Foam by a Hot Particle, Comb. Flame 162: 4112–4118 (2015).
111. Wang S, Huang X, Chen H, and Liu N, Interaction between Flaming and Smouldering in Hot-particle Ignition of Forest Fuels and Fffects of Moisture and Wind, Int. J. Wildland Fire 26: 71–81 (2017).
112. Zvyagils'kaya AI and Subbotin AN, "Influence of Moisture Content and Heat and Mass Exchange with the Surrounding Medium on the Critical Conditions of Initiation of Surface Fire," Combustion, Explosions, and Shock Waves 32: 558–564 (1996).
113. Grishin AM, Dolgov AA, Zima VP, Kryuchkov DA, Reino VV, Subbottan AN, and Tsvyk RS, "Ignition of a Layer of Combustible Forest Materials," Combustion, Explosions, and Shock Waves 34: 613–620 (1998).\
114. Matvienko OV, Kasymov DP, Filkov AI, Daneyko OI and Gorbatov DA "Simulation of fuel bed ignition by wildland firebrands" International Journal of Wildland Fire, 27, 550 (2018).
115. Lautenberger C, and Fernandez-Pello AC, "Modeling Ignition of Combustible Fuel Beds by Embers and Heated Particles," Forest Fires 2008.

116. McGrattan K, Hostikka S, Floyd J, Baum H, and Rehm R, “Fire Dynamics Simulator (Version 5) Technical Reference Guide,” NIST Special Publication 1019–5, 2007.
117. Lautenberger C “Gpyro - Generalized Pyrolysis Model for Combustible Solids “
118. Yin P, Liu N, Chen H, Lozano JS, and Shan Y, “New Correlation Between Ignition Time and Moisture Content for Pine Needles Attacked by Firebrands,” Fire Technol, vol. 50, pp. 79–91, 5 2012.
119. Jolly WM, Mcallister S, Finney MA, and Hadlow A, “Time to ignition is influenced by both moisture content and soluble carbohydrates in live Douglas fir and Lodgepole pine needles,” in Proceedings of the VI International Conference on Forest Fire Research, 2010.
120. Jolly WM et al., “Relationships between moisture, chemistry, and ignition of Pinus contorta needles during the early stages of mountain pine beetle attack,” For. Ecol. Manage, vol. 269, pp. 52–59, 2012.
121. Manzello SL and Suzuki S, Generating Firebrand Showers Characteristic of Burning Structures, Proceedings of the Combustion Institute, 36: 3247–3252, 2017.
122. Suzuki S and Manzello SL, ‘Experiments to Prove the Scientific-Basis for Laboratory Standard Test Methods for Firebrand Exposure’, Fire Safety Journal), Vol. 91 (2017) pp. 784–790.
123. Manzello SL, Hayashi Y, Yoneki T, and Yamamoto Y, Quantifying the Vulnerabilities of Ceramic Tile Roofing Assemblies to Ignition during a Firebrand Attack, Fire Safety Journal, 45:35–43, 2010.
124. L Manzello S, Park S, Suzuki S, Shields J, and Hayashi Y, Experimental Investigation of Structure Vulnerabilities to Firebrand Showers, Fire Safety Journal, 46: 568–578, 2011.
125. Manzello SL, Suzuki S, and Hayashi Y, Exposing Siding Treatments, Walls Fitted with Eaves, and Glazing Assemblies to Firebrand Showers, Fire Safety Journal, 50: 25–34, 2012.
126. Manzello SL, Suzuki S, and Hayashi Y, Enabling the Study of Structure Vulnerabilities to Ignition from Wind Driven Firebrand Showers: A Summary of Experimental Results, Fire Safety Journal, 54:181–196, 2012.
127. Suzuki S, Manzello SL, Kagiya K, Suzuki J, and Hayashi Y, Ignition of Mulch Beds Exposed to Continuous Wind Driven Firebrand Showers, Fire Technology, 51:905–922, 2015.
128. Suzuki S, Johnsson E, Maranghides A, and Manzello SL, Ignition of Wood Fencing Assemblies Exposed to Continuous-Wind Driven Firebrand Showers, Fire Technology, 52: 1051–1067, 2016.
129. Manzello SL, Suzuki S, and Nii D, Full-Scale Experimental Investigation to Quantify Building Component Ignition Vulnerability from Mulch Beds Attacked by Firebrand Showers, Fire Technology, 53: 535–551, 2017 [PubMed: 28184098]
130. Manzello SL and Suzuki S, Experimental Investigation of Wood Decking Assemblies Exposed to Firebrand Showers, Fire Safety Journal, 92: 122–131, 2017. [PubMed: 28890598]
131. Suzuki S, Nii D, and Manzello SL, The Performance of Wood and Tile Roofing Assemblies Exposed to Continuous Firebrand Assault, Fire and Materials Journal, 41: 84–96, 2017.
132. Suzuki S, and Manzello SL, Initial Study on Thatched Roofing Assembly Ignition Vulnerabilities to Firebrand Showers, Fire Safety J. 103: 34–37 (2019)
133. Manzello SL, Almand K, et al., FORUM Position Paper The Growing Global Wildland Urban Interface (WUI) Fire Dilemma: Priority Needs for Research, Fire Safety J. 100:64–66 (2018)

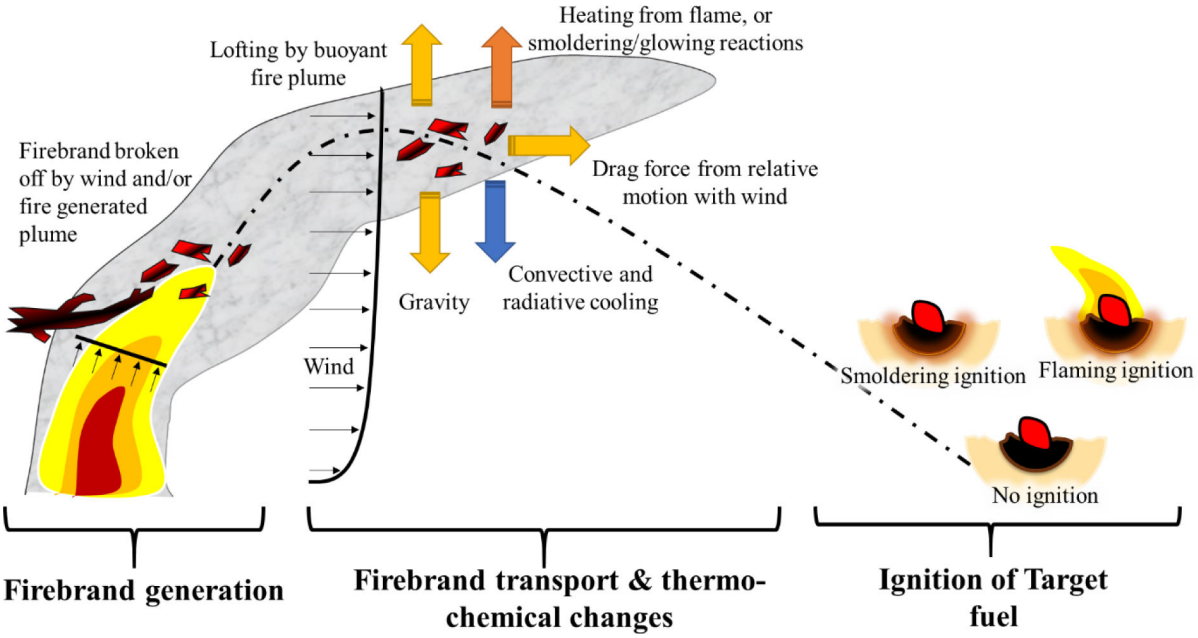

Fig. 1.

Firebrand sub-processes: (1) the generation of the firebrand, (2) coupled transport and thermo-chemical change, and (3) the potential target fuel ignition.

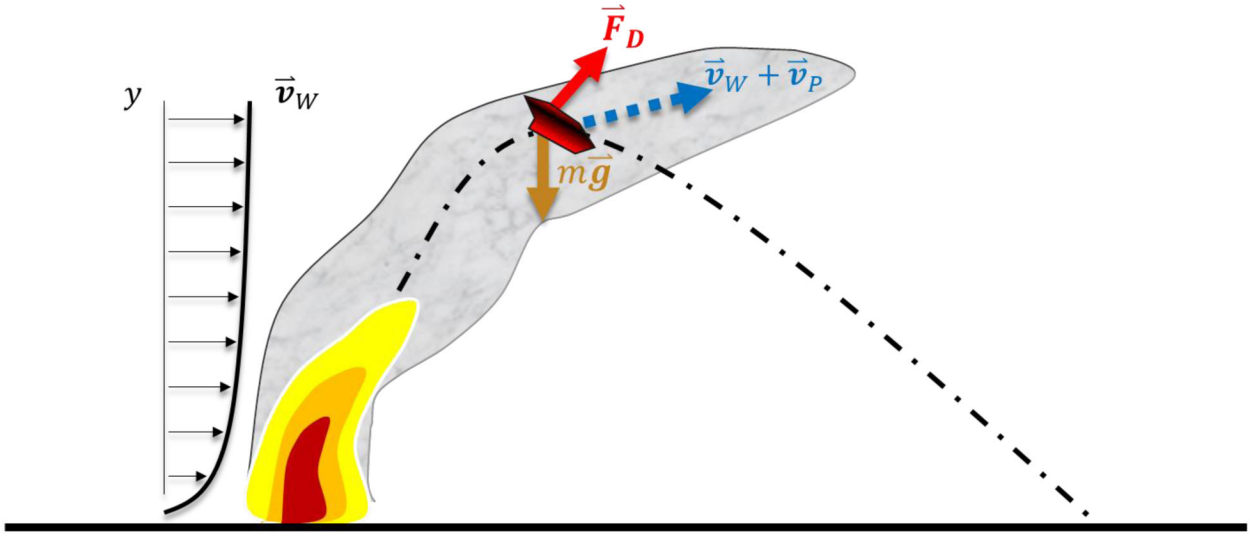

Fig. 2.
Schematic of firebrand trajectory formulation.

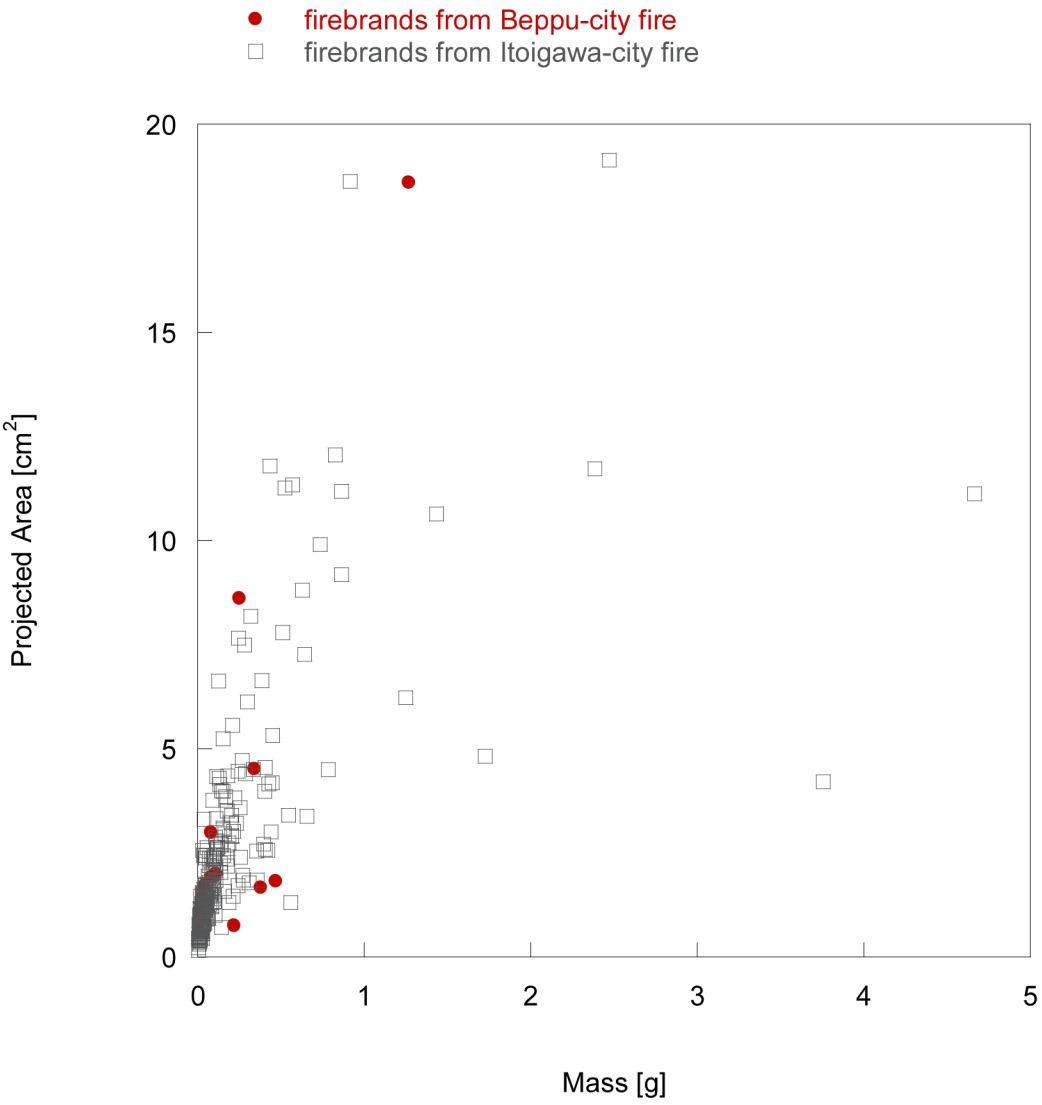

Fig.3.

Comparison with firebrand data from Itoigawa-city fire [10] and Beppu-city fire [24]. Five firebrands with the project area bigger than 20 cm^2 are omitted from this graph to focus on the smaller firebrands.

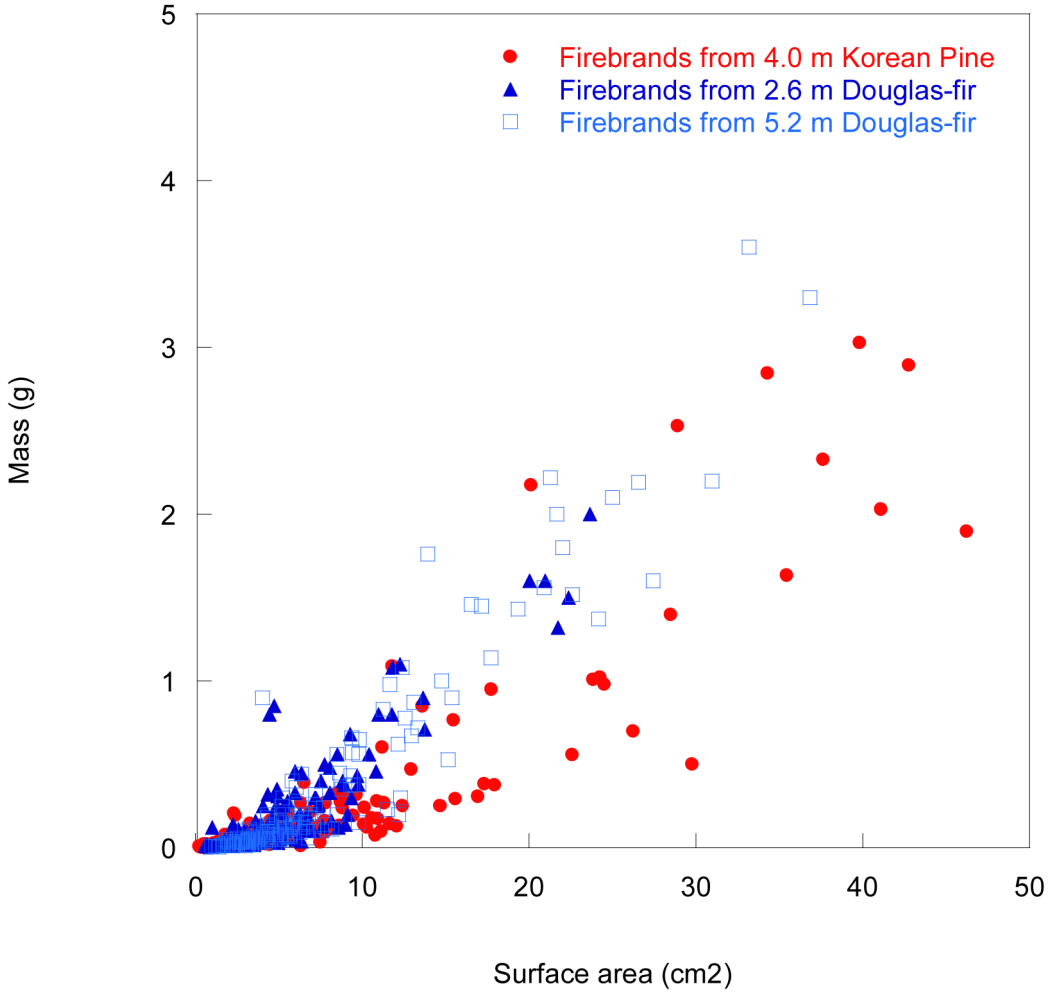

Fig. 4.
A comparison of firebrand data collected from tree combustion [17, 33].

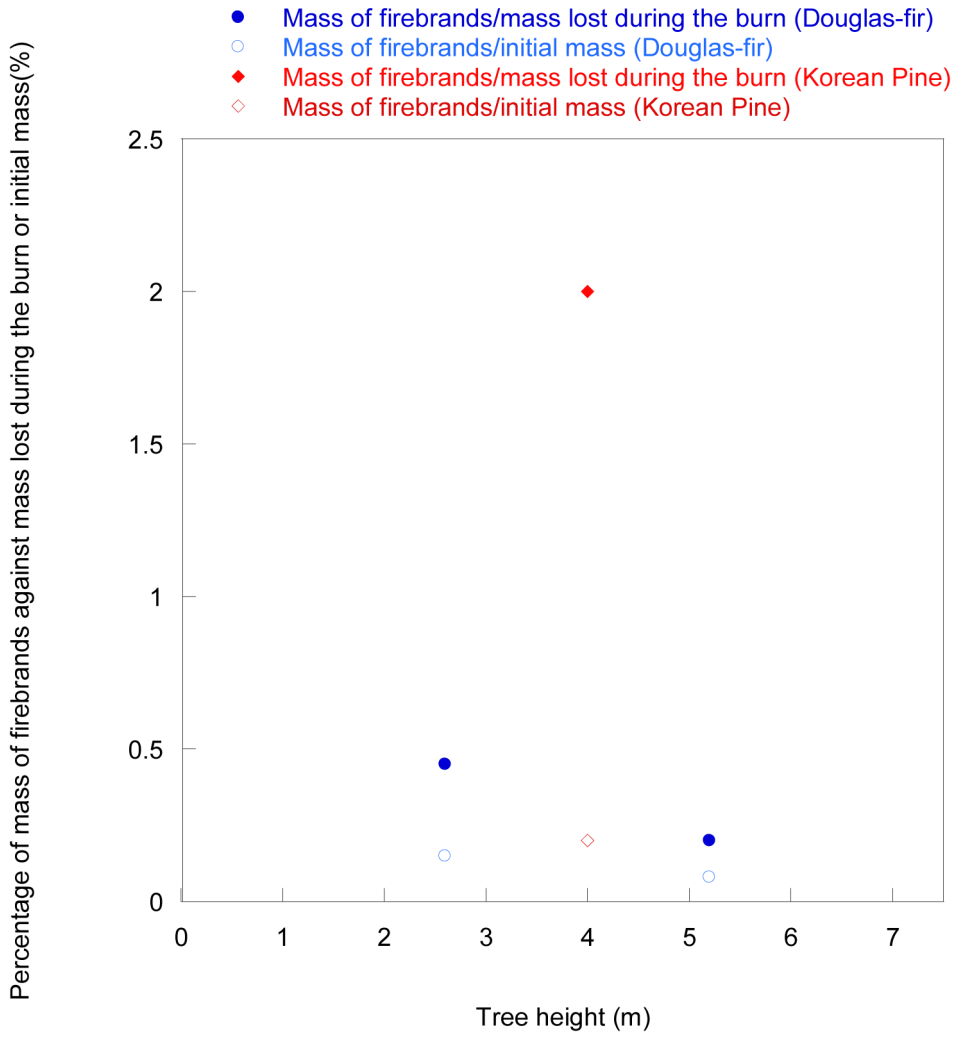

Fig. 5.

The total mass of firebrands produced from each tree size was normalized with the mass loss of a tree during the burn as well as initial mass of a tree [33].

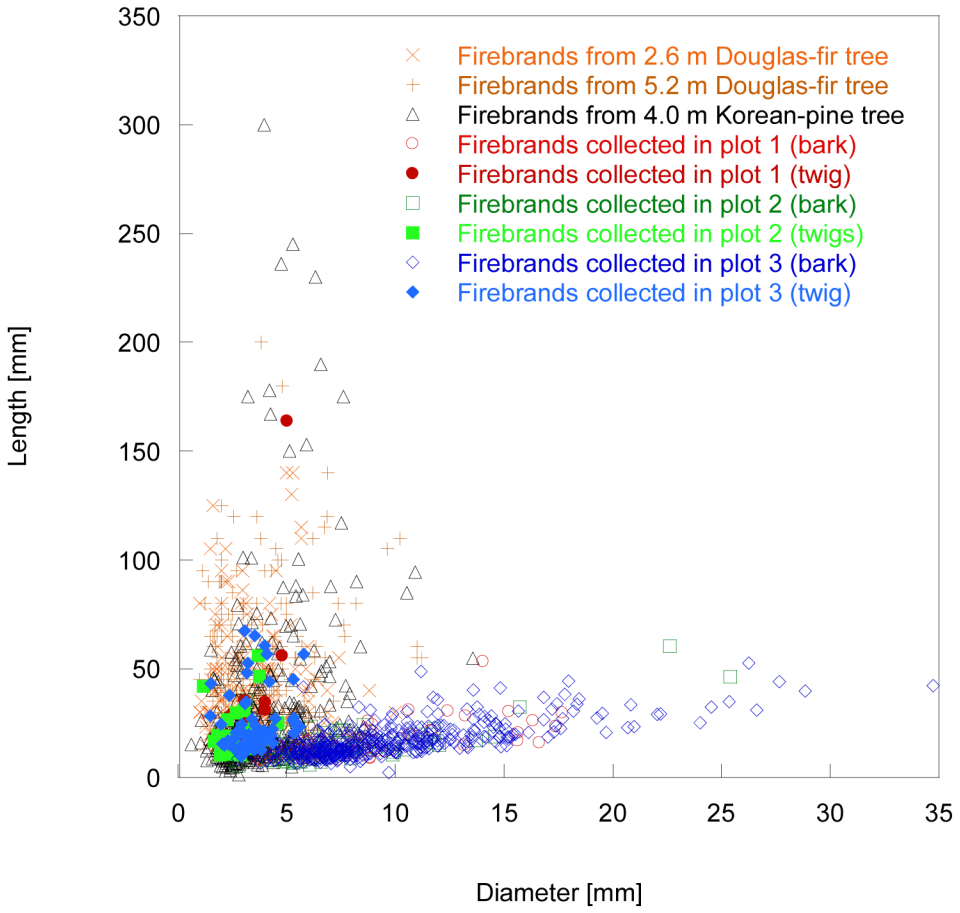

Fig. 6.

Comparison of firebrand data collected from simple individual tree combustion to those collected from field scale burns. [17, 31, 35]

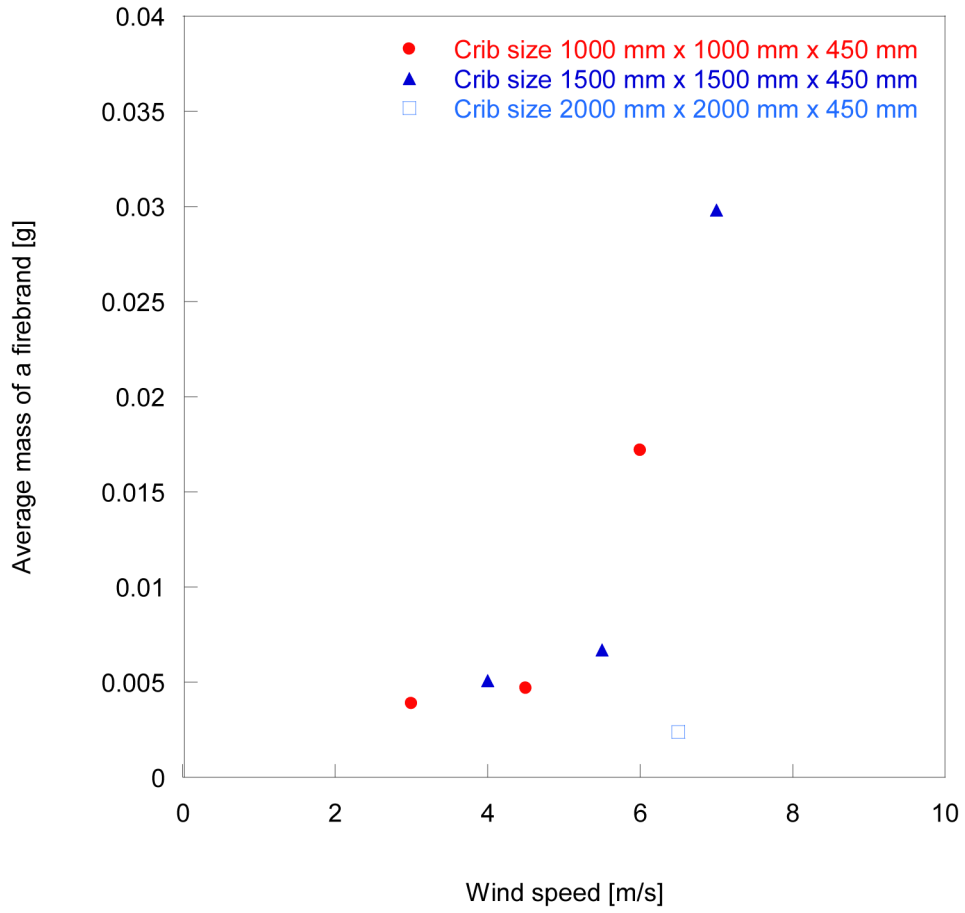

Fig. 7.
Firebrand data collected from burning cribs [42].

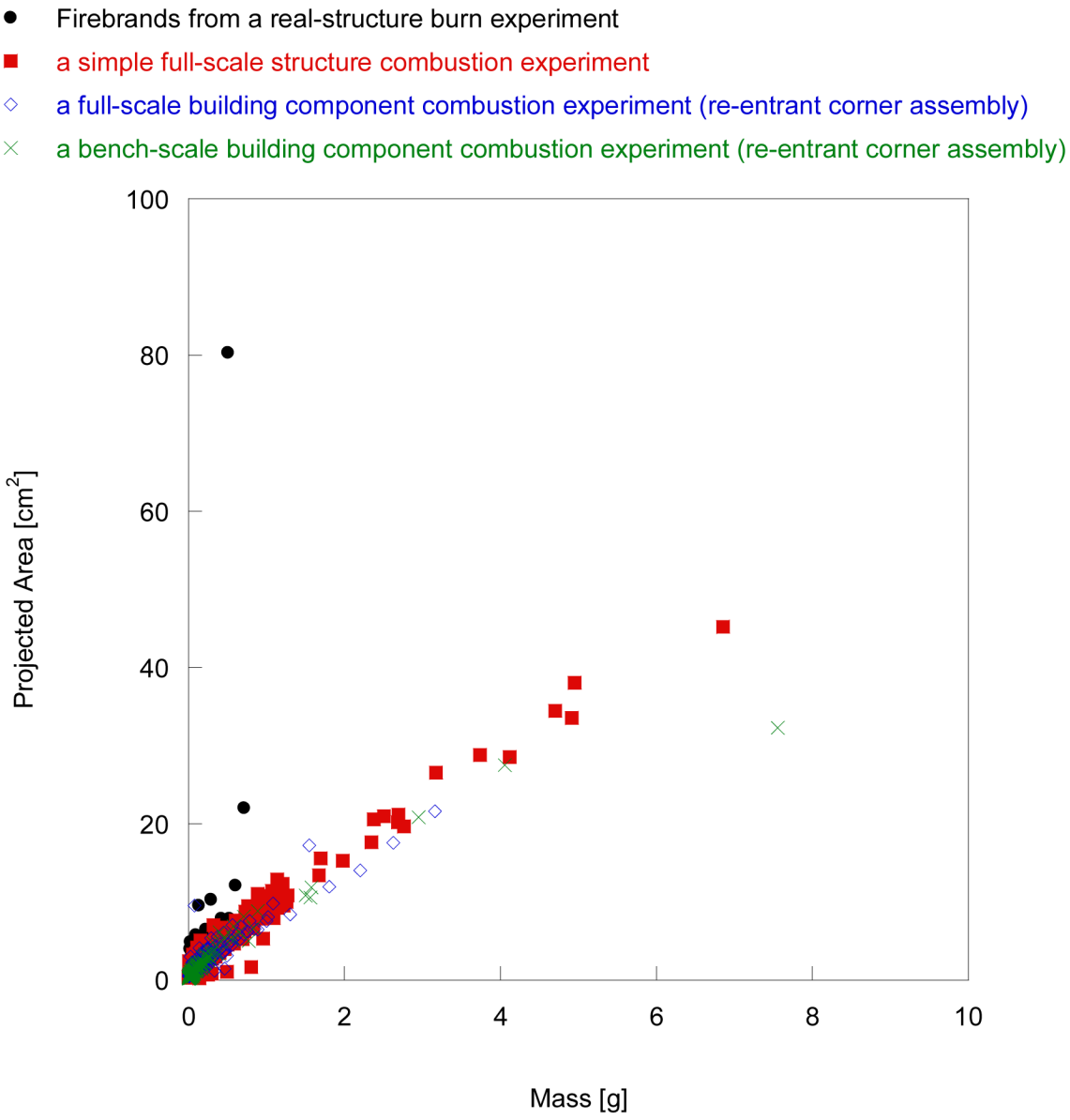

Fig. 8.

Comparison of firebrand data collected from a real-structure burn experiment [48], a full-scale structure combustion experiment [49], a full-scale building component combustion experiment [50] and a bench-scale building component combustion experiment [53]. (all under a 6 m/s wind condition).

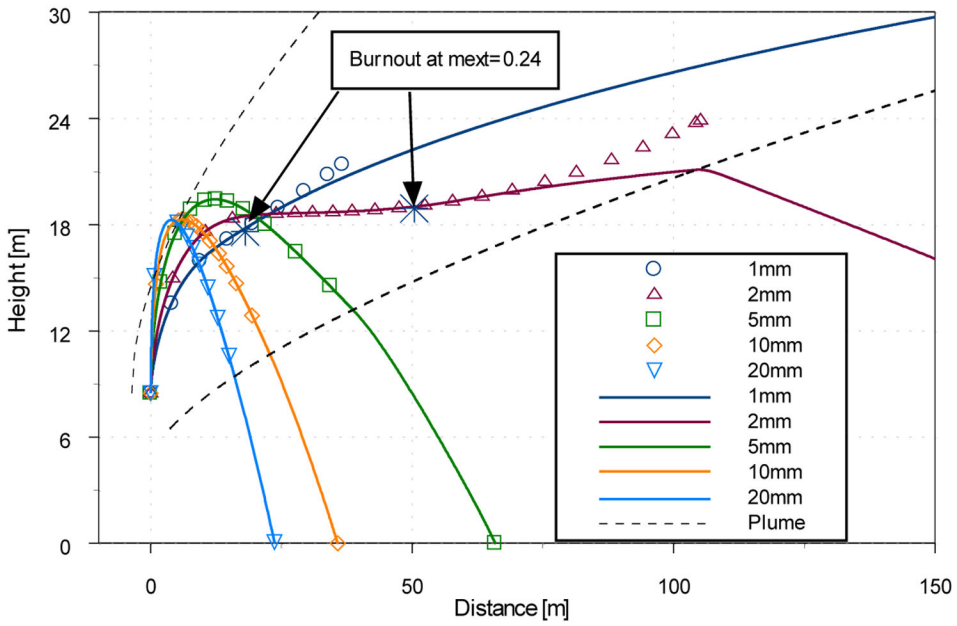

Fig. 9.

An example of firebrand trajectory cylinders in the buoyant plume of a 40MW fire and a 48 km/hr wind [79].

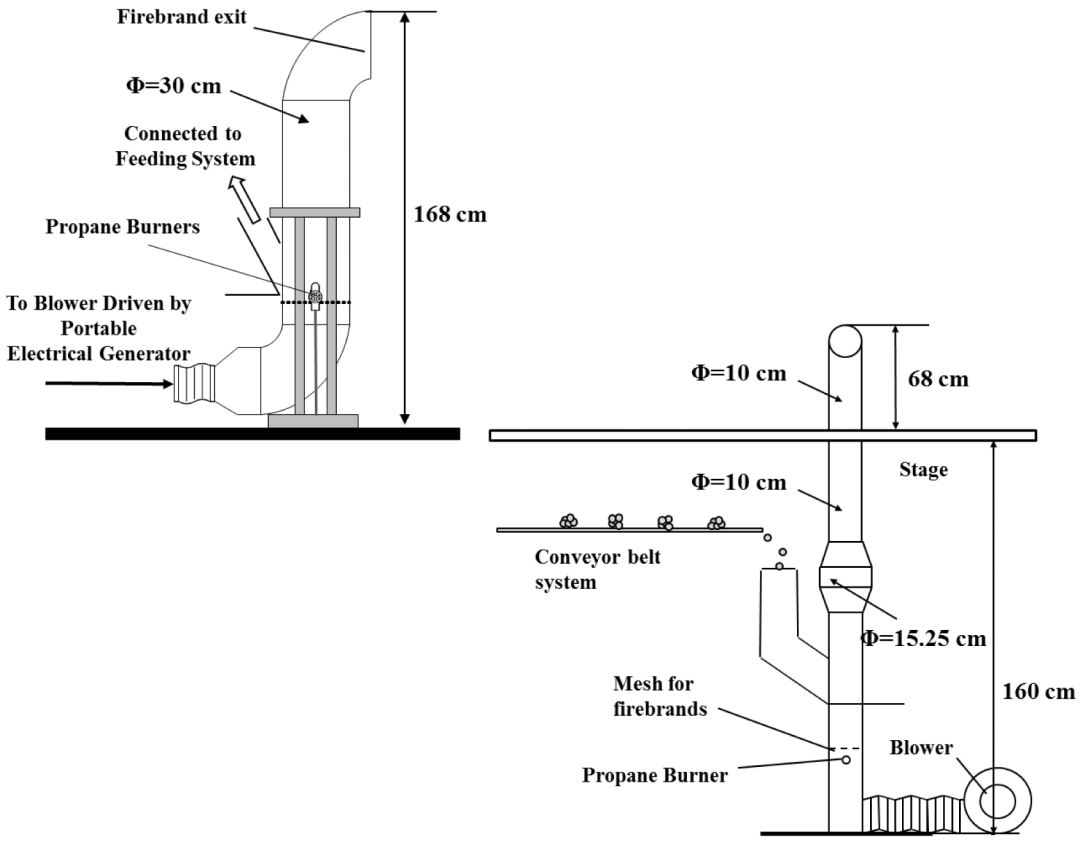

Fig. 10.

A comparison of the full-scale (left hand side) and reduced-scale firebrand generators [122].

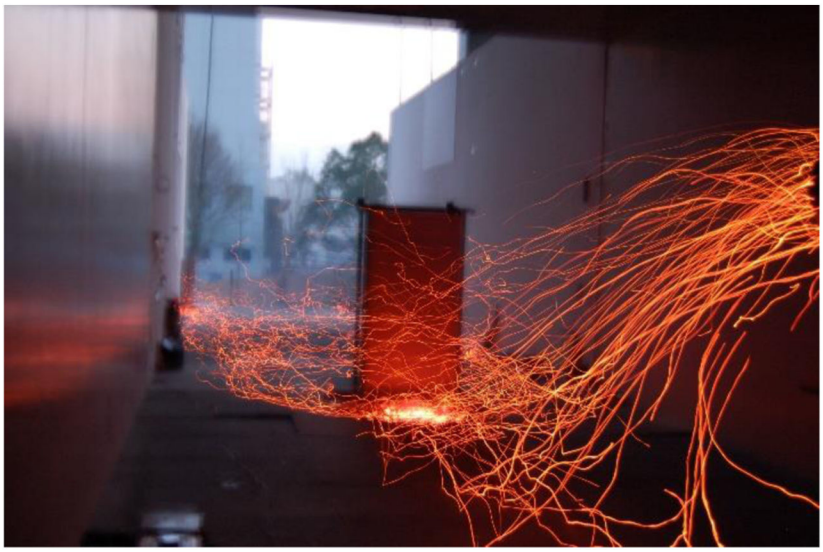

Fig. 11.
Firebrands generated by the NIST Dragon inside the Fire Research Wind Tunnel Facility [124].

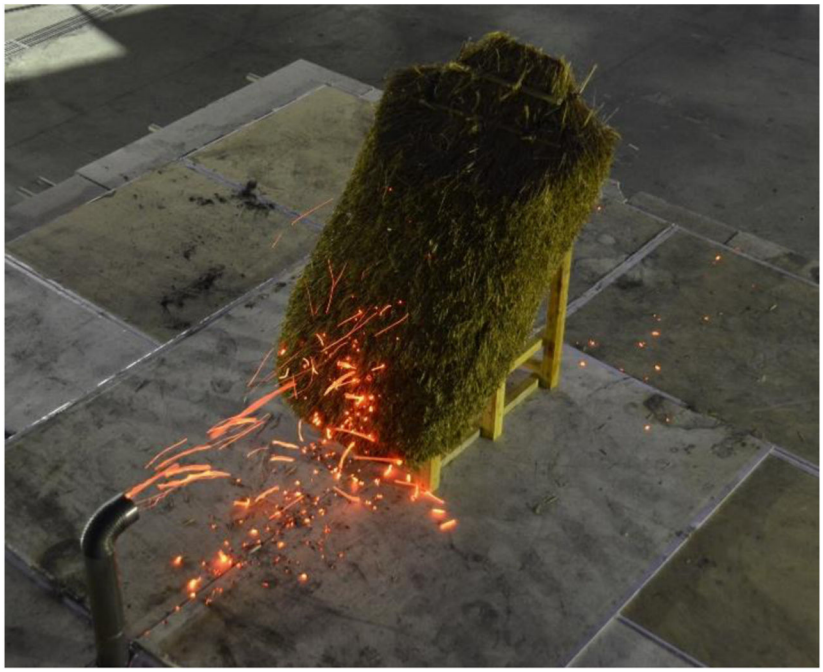

Fig. 12.
Thatched roofing assembly (mock-up) exposed to wind-driven firebrand showers characteristic to those generated from structure combustion [132].

Table 1

Summary of firebrand density (m^{-2}) collected in prescribed burns over years with projected area of more than 5×10^{-5} m^2 (density for 2016 was recalculated) Collection methods are same for 2013 and 2014 but different for 2016. FCS X, Y, Z indicates the locations where firebrands were collected.

	2013			**2014**			**2016**		
	plot 1	**plot 2**	**plot 3**	**plot 1**	**plot 2**	**plot 3**	**FCS X**	**FCS Y**	**FCS Z**
firebrand density in the collection container (m^{-2})	60	44	238	12	960	39	71	111	123

Table 2

Experimental Matrix for crib as surrogate of structures [42].

Crib size	repeat	Wind speed (m/s)	Average mass of firebrands (g)
1000 mm × 1000 mm × 450 mm	3	3	0.0039
	3	4.5	0.0047
	3	6	0.0172
1500 mm × 1500 mm × 450 mm	2	4	0.0051
	2	5.5	0.0067
	2	7	0.0298
2000 mm × 2000 mm × 450 mm	1	6.5	0.0024

Table 3

The number of firebrands and the average mass of firebrands from different experimental conditions [46].

	Collection methods	wind speed (m/s)	Structural information	average mass (g)	Projected area (cm^2)					
					0.25 to 1	1 to 2	2 to 4	4 to 9	9 to 25	More than 25
Case 1	Watered floor	2	Japanese style fire prevention house (mortar & tile roof)	0.14	21	35	35	16	0	0
Case 2	Wet pan	6	Japanese style fire prevention house (mortar & tile roof)	N/A	many	many	173	48	12	3
	Dry pan			0.0719	64	105	45	14	0	0
Case 3	Wet pan	4	Western style house (sidings and slate roof)	0.0170	308	44	15	1	0	0
	Dry pan			0.0620	33	15	10	4	0	0